Journal of Renewable and Sustainable Energy

REVIEW ARTICLE | OCTOBER 15 2024

Modeling and observations of North Atlantic cyclones: Implications for U.S. Offshore wind energy

Jiali Wang ; Eric Hendricks ; Christopher M. Rozoff ; Matt Churchfield ; Longhuan Zhu ; Sha Feng ; William J. Pringle; Mrinal Biswas ; Sue Ellen Haupt ; Georgios Deskos ; Chunyong Jung; Pengfei Xue ; Larry K. Berg ; George Bryan ; Branko Kosovic ; Rao Kotamarthi

J. Renewable Sustainable Energy 16, 052702 (2024)
https://doi.org/10.1063/5.0214806

Journal of Renewable and Sustainable Energy REVIEW pubs.aip.org/aip/rse

Modeling and observations of North Atlantic cyclones: Implications for U.S. Offshore wind energy

Cite as: J. Renewable Sustainable Energy **16**, 052702 (2024); doi: 10.1063/5.0214806
Submitted: 19 April 2024 · Accepted: 27 August 2024 ·
Published Online: 15 October 2024

View Online Export Citation CrossMark

Jiali Wang,[1,a)] Eric Hendricks,[2] Christopher M. Rozoff,[2] Matt Churchfield,[3] Longhuan Zhu,[4,b)] Sha Feng,[6] William J. Pringle,[1] Mrinal Biswas,[2] Sue Ellen Haupt,[2] Georgios Deskos,[3] Chunyong Jung,[1] Pengfei Xue,[1,4,5] Larry K. Berg,[6] George Bryan,[2] Branko Kosovic,[2] and Rao Kotamarthi[1]

AFFILIATIONS

[1]Environmental Science Division, Argonne National Laboratory, Lemont, Illinois 60439, USA
[2]U.S. National Science Foundation National Center of Atmospheric Research, Boulder, Colorado 80307, USA
[3]National Wind Technology Center, National Renewable Energy Laboratory, Golden, Colorado 80401, USA
[4]Great Lakes Research Center, Michigan Technological University, Houghton, Michigan 49931, USA
[5]Department of Civil, Environmental and Geospatial Engineering, Michigan Technological University, Houghton, Michigan 49931, USA
[6]Atmospheric, Climate, and Earth Sciences (ACES) Division, Pacific Northwest National Laboratory, Richland, Washington 99352, USA

[a)]**Author to whom correspondence should be addressed:** jialiwang@anl.gov
[b)]**Present address:** School of Marine Science and Ocean Engineering, University of New Hampshire, New Hampshire 03824, USA

ABSTRACT

To meet the Biden-Harris administration's goal of deploying 30 GW of offshore wind power by 2030 and 110 GW by 2050, expansion of wind energy into U.S. territorial waters prone to tropical cyclones (TCs) and extratropical cyclones (ETCs) is essential. This requires a deeper understanding of cyclone-related risks and the development of robust, resilient offshore wind energy systems. This paper provides a comprehensive review of state-of-the-science measurement and modeling capabilities for studying TCs and ETCs, and their impacts across various spatial and temporal scales. We explore measurement capabilities for environments influenced by TCs and ETCs, including near-surface and vertical profiles of critical variables that characterize these cyclones. The capabilities and limitations of Earth system and mesoscale models are assessed for their effectiveness in capturing atmosphere–ocean–wave interactions that influence TC/ETC-induced risks under a changing climate. Additionally, we discuss microscale modeling capabilities designed to bridge scale gaps from the weather scale (a few kilometers) to the turbine scale (dozens to a few meters). We also review machine learning (ML)-based, data-driven models for simulating TC/ETC events at both weather and wind turbine scales. Special attention is given to extreme metocean conditions like extreme wind gusts, rapid wind direction changes, and high waves, which pose threats to offshore wind energy infrastructure. Finally, the paper outlines the research challenges and future directions needed to enhance the resilience and design of next-generation offshore wind turbines against extreme weather conditions.

SIGNIFICANCE STATEMENT

To achieve the Biden-Harris administration's goal of setting up 30 GW of offshore wind power by 2030 and aiming for 110 GW by 2050, it is important to build wind farms in U.S. waters that have high wind energy potential. However, these areas often face hurricanes and big storms. Understanding the risks these storms pose and building strong, reliable wind farms are key. This paper reviews the tools and methods used to study these storms and their effects on wind farms and turbines. It looks at how well different models can predict the impact of storms on the ocean and atmosphere, important for designing safer wind turbines. We also discuss newer methods, like using machine learning, to predict storm effects at different scales—from large weather patterns down to individual turbines. The paper highlights the tough conditions like very strong winds and big waves that can damage wind farms. It stresses the need for more research to make wind turbines that can withstand these extreme conditions.

I. MOTIVATION

The combined offshore wind energy potential of the United States along the coasts of the North Atlantic, the Gulf of Mexico, and

Hawaii exceeds 1000 GW (Musial *et al.*, 2020). However, exposure to extreme weather conditions limits deployment opportunities due to a number of turbine design challenges. For example, offshore wind turbines (OWTs) sited along the eastern coast of the United States and Gulf of Mexico can be vulnerable to major tropical cyclones (TCs, such as hurricanes of Category 3 and above on the Saffir–Simpson intensity scale). In addition, as TCs travel into higher latitudes, they often interact with midlatitude systems such as upper-level troughs or extratropical cyclones (ETCs) and transform from a symmetric, warm-core tropical system to an asymmetric, cold-core extratropical system (Jones *et al.*, 2003; Evans *et al.*, 2017). This process, referred to as extratropical transition (ETT), involves modifications to the TC itself such as the expansion of the asymmetric distribution of wind and precipitation, impacting a wider area as it transitions. This implies that the risks associated with tropical storms remain significant even in the midlatitudes, such as the northeastern continental shelf of the United States and offshore. Both TCs and ETCs can produce extreme wind gusts, high waves, heavy precipitation, and frequent and intense lightning. These hazardous conditions may affect an entire OWT, including its blades, tower, foundations, and associated substations. However, the nature of extreme weather makes it difficult to assess the true vulnerability of OWTs, because historical records and measurements of the extreme weather loadings may be limited. For example, hundreds of OWTs (80%) in the North Sea required extensive repairs because weather extremes exceeded predictions (Diamond, 2012).

Although global offshore wind has a deployed capacity approaching 50 GW, more than half of this capacity is in Europe, where there is no major hurricane risk. Almost all of the remainder of this capacity is installed in Asia, but these OWT arrays are still too recent to provide sufficient data for studying the impacts of major TCs on installation, operation, and maintenance of OWTs. To meet the Biden-Harris administration goal to deploy 30 GW of offshore wind energy by 2030 and set the nation on a path to 110 GW or more by 2050, robust risk assessments are greatly needed offshore of the United States. Turbines and their support structures must be able to withstand high loads that may occur due to various conditions. These include extreme microscale turbulence, high wave conditions, storm surge, wind/wave misalignment, and, more generally, low-cycle fatigue. Low-cycle fatigue results from repeated buffeting or loads outside of buffeting. Additionally, these structures must endure other events involving complex combinations of these external load drivers. The current design approach is based on wind turbine standards established by the International Electrotechnical Commission (IEC). For aerodynamic load analysis, a Tropical Class turbine (T-turbine) is defined on the assumption that only the reference 10-min average wind speed, needs to be adjusted from 50 to 57 m s^{-1}. Similarly, in TC-affected regions, an additional subset of marine conditions related to the wave and combined wave/current design loads have been recommended by the standards (IEC, 2019). Although these updates and recommendations for the design standard may ultimately require turbine designers to strengthen blades, towers, and other components, their simplicity still ignores the actual complexity of a hurricane event and the possibility that other damaging design load cases might exist (as listed above). For example, site-specific assessments are unavailable in these standards but are greatly needed to determine the reference wind and wave parameters that are unique to a certain region. An additional challenge is assessing how the changing climate will affect these extreme events beyond the next two decades (over an offshore turbine's ∼20-year operational life cycle), given that the observation data shows a statistically significant increasing trend for the intensity and the impacts of severe hurricanes over the North Atlantic (Knutson *et al.*, 2007).

As a first step toward developing a more complete picture of the impact of TCs and ETCs on U.S. offshore wind energy, this study conducted a comprehensive review of the state-of-the-art and existing literature. Specifically, as outlined in Fig. 1, we describe current observational capabilities (Sec. II) and current state-of-the-science modeling of these extreme events at the Earth system scale, mesoscale or weather scale, microscale or turbine scale (Sec. III), plus the use of artificial intelligence (AI) and machine learning (ML) for generating TC/ETC associated extremes (Sec. IV) efficiently for OWT risk assessment. Section V reviews projected changes in TC/ETC in future climate using various modeling approaches. Risk assessment is described in Sec. VI. Section VIII enumerates gaps in our scientific knowledge.

II. CURRENT OBSERVATIONAL CAPABILITIES

OWTs are affected by winds through the rotor swept area, precipitation, and wave action. In this section, we describe the current state of satellite and *in situ* measurements within TC boundary layers that measure these quantities. The information in this summary is provided by Topic 1 of the Tenth International Workshop on Tropical Cyclones held in 2022 (Ricciardulli and Howell, 2022; Holbach and Bousquet, 2022; Wimmers and Duong, 2022; and Herndon and Langlade, 2022). National Oceanic and Atmospheric Administration (NOAA) and the U.S. Air Force routinely send operational reconnaissance aircrafts into TCs in the North Atlantic to measure intensity and structure. These flights become more frequent when a given TC threatens to make landfall. The aircraft typically measure flight-level winds (usually at 700 hPa) directly and near-surface winds remotely using the Stepped-Frequency Microwave Radiometer. Dropsondes are released at the radius of maximum winds and in the eye to obtain vertical profiles of temperature, pressure, and winds from the surface to flight level. NOAA aircraft are equipped with tail Doppler radars, which are used to create three-dimensional wind and reflectivity analyses at synoptic time scales (i.e., 6-h intervals). In addition to the operational flights, research missions by government agencies and industry are also conducted during the North Atlantic hurricane season, with a variety of different measurement platforms. A relevant platform to this study is the Imaging Wind and Rain Airborne Profiler, which measures ocean height, significant wave height, and three-dimensional wind and reflectivity profiles from below the aircraft (700 hPa or approximately 3000 m above sea level) to the surface. In addition, lidars have been deployed on aircraft during research missions, such as the Airborne Doppler Wind Lidar; these have higher vertical resolution than radars (∼50 m). From 2015 to 2016, wind profiles from this instrument were obtained in several hurricanes from 25 m to 7 km above sea level, with the most frequent measurements between 1500 and 2000 m (Bucci *et al.*, 2018; Zhang *et al.*, 2018).

In recent years, a number of new platforms have begun taking measurements of the upper ocean and support analyzing and forecasting TC intensity, structure, track, and their associated hazards (Holbach *et al.*, 2023). Underwater gliders can take measurements to a depth of 1000 m at high-temporal frequency. Ocean profilers (e.g., bathythermographs) are deployed from aircraft to measure the thermal structure of the upper ocean. Deployed through the Argo program, Autonomous Profiling Explorer floats routinely measure the upper

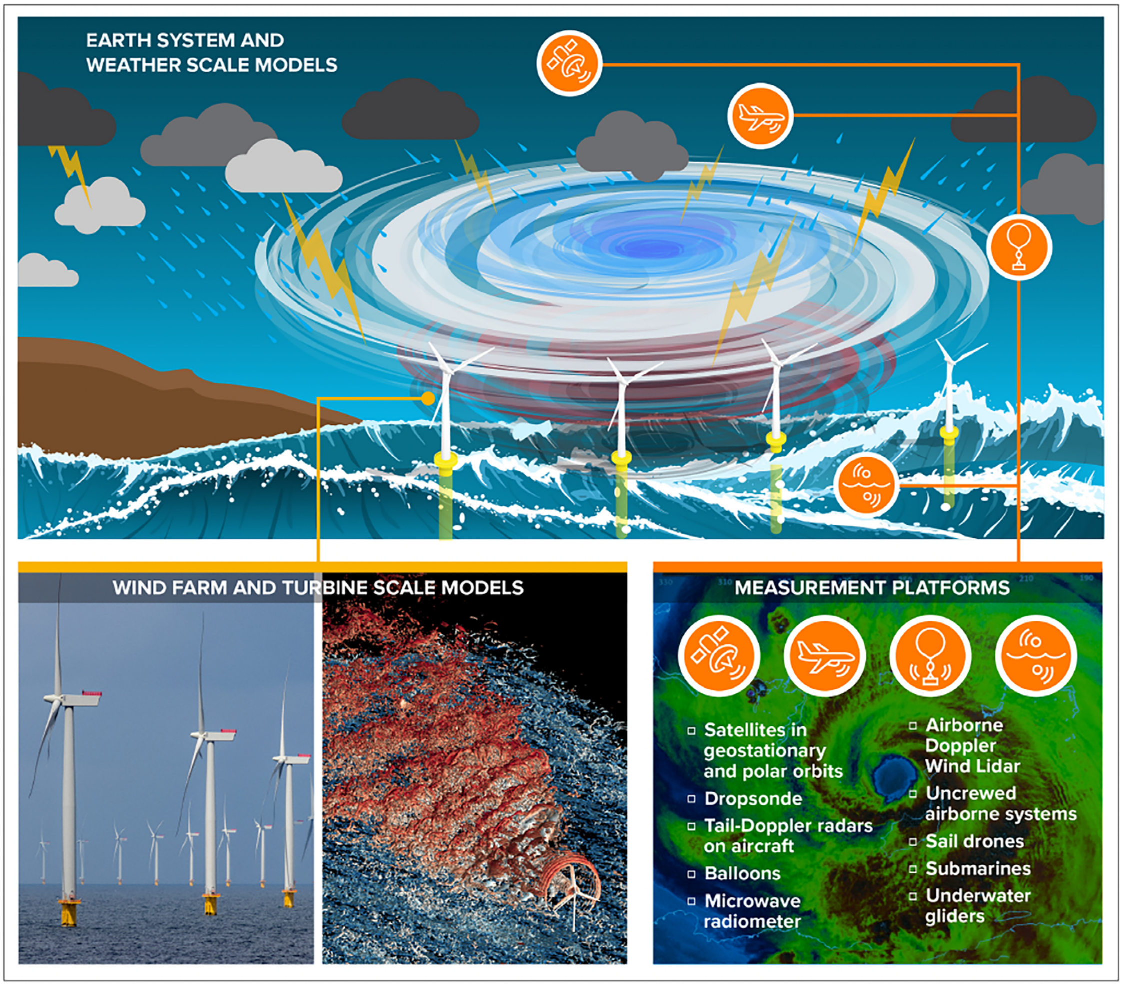

FIG. 1. A conceptual overview of the modeling and measurement tools used to analyze offshore weather conditions during storm events.

ocean and its response to hurricane passages. The Wide Swath Radar Altimeter measures significant wave height, wavelength, propagation direction, and wave spectra. The Ka-band interferometric radar measures ocean height and low to moderate wind speeds. Similarly, new observational platforms have been developed for probing the TC boundary layer. Uncrewed airborne systems (UASs) have been deployed from reconnaissance aircrafts to take wind, pressure, and temperature measurements in the boundary layer. One finding of these UASs is the existence of extreme wind gusts that can significantly exceed the best-track hurricane intensity. Uncrewed sail drones are used to sample the upper ocean and near-surface underneath the hurricane eyewall. Balloons (e.g., Aeroclippers) have been deployed to loiter for long periods of time and take low-level wind measurements, although their movement is not controlled. If deployed in the right place at the right time, the balloons can move with the low-level winds into the eyewall and eye regions. Global sounding balloons can fly for weeks and vertically profile the atmosphere from 200 m to 20 km above the surface.

Satellites in geostationary and polar orbits routinely take a variety of TC-related measurements that allow inferences about a TC's intensity and structure. Moreover, satellites provide sufficient information to characterize important aspects of a TC's boundary layer. Synthetic aperture radars (SARs) measure the ocean surface at very high resolution (50–100 m), and backscatter can be used to infer the near-surface wind field of the TC. They can retrieve measurements of winds up to approximately 70 m s^{-1}. L-band radiometers can retrieve winds with coarser spatial resolutions of 40–50 km, although the main advantage of L-band radiometers is the wider swath (1000 km) and more continuous measurements than SARs. In a similar vein, the large swath of scatterometers (1000 km) can be used to map the TC outer wind field. Microwave imagers provide TC centers, cloud pattern/precipitation information, wind speed, and sea surface temperatures (SSTs). The new generation of geostationary satellites (e.g., Himawari-8/9) provide much higher temporal resolutions (10 min for the full disk, and 2-min frequencies for targeted locations) than previous satellites. Recently, small and cube satellites have extended the spatial and temporal coverage of wind measurements over Earth. One recent example is the National Aeronautics and Space Administration's Cyclone Global Navigation Satellite System constellation, which measures ocean surface winds.

The NOAA Hurricane Research Division maintains an archive of datasets discussed in this review section, specifically for North Atlantic and eastern North Pacific TCs, accessible at https://www.aoml.noaa.gov/data-products/. Operational warning centers, such as the National Hurricane Center, employ both *in situ* and satellite measurements to generate objective analyses of tropical cyclones. These analyses facilitate the determination of key metrics, including the maximum 1-min sustained wind speed and various wind radii, encompassing the radius of maximum winds as well as the extents of winds reaching 34, 50, and 64 knots.

III. PHYSICS AND NUMERICAL MODELING STUDIES

Over the last two decades, there has been steady improvement in TC track forecasting, mostly due to improvements in dynamical models, better assimilation of satellite data, improved model physics, and increased resolution. However, improvement in TC intensity prediction has been slower (Cangialosi, 2023; Wada and Usui, 2010). Cangialosi (2023) demonstrated that over the past three decades (1990–2022), the 24–72-h track forecast errors in the North Atlantic basin have been reduced by about 75%, while the 48-h intensity forecast errors decreased by 30%. Previous numerical studies based on coupled atmosphere–ocean simulations or forecasts from world leading agencies such as Integrated Forecast System (IFS) of European Center for Medium-Range Weather Forecasts (ECMWF) (Mogensen *et al.*, 2017), Non-Hydrostatic Model of Japan Meteorological Agency (Wada *et al.*, 2018), Global/Regional Assimilation and PrEdiction System (GRAPES) of China Meteorological Administration (Zhang and Shen, 2008), Hurricane Weather Research and Forecasting (HWRF) of NOAA (Bernardet *et al.*, 2015; Mehra *et al.*, 2018), and Geophysical Fluid Dynamics Laboratory (GFDL) regional coupled model of NOAA (Bender and Ginis, 2000) have demonstrated the important role of ocean coupling in TC intensity prediction. Benefitting from an interactive ocean model and data assimilation, weak TCs in ECMWF Reanalysis version 5 (ERA5) (Hersbach *et al.*, 2020) were well reproduced. However, challenges remain, and the operational numerical models tend to underestimate strong TCs (Yamaguchi *et al.*, 2017) mainly due to coarse grid spacing, poor formulations of the surface and boundary layers, and insufficient understanding of the coupled ocean–atmosphere system (Chen *et al.*, 2007). Sections III A–III C review the research progress of physics numerical modeling at global and regional scales to the wind farm and even wind turbine scales. Particular attention is given to the models' capability to realistically simulate the TC and ETC and their associated extreme winds and waves through high spatial resolutions and multi-way interactions between atmosphere, ocean, and waves.

A. Earth system models

Earth system models are useful tools for studying various aspects of TCs. These model help analyze changes in frequency and geographical distribution, the role of ocean–atmosphere interactions, and project future TC activity under different greenhouse gas emission scenarios. TCs develop and evolve over a wide range of spatiotemporal scales: convective processes within a storm's core occur within a few kilometers, while the larger environment influencing TCs spans tens of thousands of kilometers. The lifespan of an individual cyclone is measured in hourly and daily timescales, though the large-scale environment impacting cyclones can vary over seasonal to decadal timescales. On subseasonal timescales, there are three main drivers that affect the North Atlantic TC and ETC activities through changing the large-scale upper-level divergence, vertical wind shear, and relative humidity. They are the convectively coupled equatorial waves (e.g., Madden–Julian Oscillation (MJO) (Madden and Julian, 1972), the quasi-biweekly oscillation (QBWO) (Krishnamurti and Bhalme, 1976), and extratropical Rossby wave breaking (RWB) events (Zhang *et al.*, 2016; Papin *et al.*, 2020), which occur at the timescale of 30–90, 10–30, and 5–15 days, respectively. On seasonal timescales, the dominant driver of global TC activity is the El Niño Southern Oscillation (Gray, 1984; Julian and Chervin, 1978), which has significant effects on North Atlantic TC activity through modulation of SSTs, atmospheric stability, and vertical wind shear. Most current Earth System Models (ESMs) use a grid spacing of approximately 100 km (Palmer, 2014; Schneider *et al.*, 2017). Although these ESMs can resolve the large-scale environment of TCs, the representation of some essential TC characteristics (e.g., intensity) is poor (Camargo, 2013). The primary cause of inaccuracies in these models stems from not adequately resolving clouds and the vertical heat transport processes. Vertical heat transport relies mainly on convection, which is not well captured at horizontal scales larger than a few kilometers (Palmer, 2014). Therefore, high-resolution climate models are necessary to accurately represent critical processes involved in TC formation and development (Camargo *et al.*, 2020). Several modeling centers have developed high-resolution general circulation models (GCMs) with the goal of improving the representation of TCs (Heming *et al.*, 2019) and have participated in the High-Resolution Model Intercomparison Project (HighResMIP) (Haarsma *et al.*, 2016) as part of the Coupled Model Intercomparison Project Phase 6 (CMIP6). Studies using these GCMs found that they can reasonably capture observed characteristics of TCs when using a grid spacing of at least 0.25° (Bacmeister *et al.*, 2014; Shaevitz *et al.*, 2014; Roberts *et al.*, 2015; Roberts *et al.*, 2020; Wehner *et al.*, 2014; Moon *et al.*, 2022; and Rendfrey *et al.*, 2021), although there are still low-intensity biases associated with models' physical parameterizations and/or dynamical cores (Reed and Jablonowski, 2011; Kim *et al.*, 2014). Balaguru *et al.* (2020) compared a fully coupled atmosphere–ocean model, Energy Exascale Earth System Model (E3SM), at low- and high-resolution (Caldwell *et al.*, 2019; Golaz *et al.*, 2019) and demonstrated that TC frequency, lifetime maximum intensities, and the relative distribution among the different basins are improved considerably in the high-resolution configuration (grid spacing of $\sim$0.25°) as opposed to the low resolution (grid spacing of $\sim$1°). In addition, ocean–atmosphere coupling in models is essential since ocean feedback to the atmosphere significantly affects TC intensity. Tsartsali *et al.* (2022) investigated the horizontal resolution dependence of ocean–atmosphere coupling along the Gulf Stream using HighResMIP protocol and found that increasing ocean and/or atmosphere resolution leads to enhanced ocean–atmosphere coupling and improved agreement with reanalysis and observations. Zhang *et al.* (2023a) used the Community ESM (CESM) at high spatial resolutions (down to 3 km for the ocean and 5 km for the atmosphere) to capture major weather–climate extremes in the atmosphere and ocean, stressing the importance of permitted clouds and ocean sub mesoscale eddies in modeling TCs and eddy–mean flow interactions. Moreover, ocean surface gravity waves are a crucial aspect of the physical processes at the atmosphere–ocean interface. The wave processes can influence momentum and energy fluxes, gas fluxes, upper ocean mixing, sea spray production, ice fracture in the marginal ice zone, and Earth albedo (Cavaleri *et al.*, 2012). Recent studies have demonstrated that incorporating aspects of surface waves into ESMs can improve skill performance, especially in simulating SST, wind speed at 10 m height, ocean heat content, mixed-layer depth, and the Walker and Hadley circulations (Law Chune and Aouf, 2018; Song *et al.*, 2012; Shimura *et al.*, 2017; Qiao *et al.*, 2013; Fan and Griffies, 2014; and Li *et al.*, 2016).

B. Mesoscale or regional-scale models

Mesoscale or regional-scale models, with higher resolution than global models, are used to gain a more detailed understanding the TC system. These models are useful for analyzing fine-scale dynamics and structure, including eye-wall formation, rain bands and wind distribution, and their interaction with local features such as coastal and inland areas. This section reviews atmosphere, ocean, and wave models collectively, which predict the dynamic and thermodynamic variables describing a TC state, including TC intensity and track, at spatial scales of a few to dozens of kilometers and over daily or smaller time scales (Ooyama, 1990). As a bottom boundary of the atmosphere, the ocean and waves have significant effects on the dynamics and thermodynamics of the atmosphere through surface roughness and heat exchange. TCs and strong ETCs impose a wind-driven wave environment upon the sea. Consequently, the surface roughness is strongly correlated with the near-surface wind speed. In this regime, over 95% of the energy from surface wind stress is transferred into the ocean, which drives strong ocean currents. The remaining energy is propagated away by waves (Sullivan and McWilliams, 2010). This energy transfer is thought to be primarily caused by the intermittent breaking of waves, which diffuses this energy from the surface via fast winds. Wave breaking may also influence the heat exchange through its generation of spray. Indirectly, wave-induced vertical mixing during TCs brings colder waters up from the subsurface, cooling the SST and dissipating the TC intensity. Processes not related to wind–wave interactions can also affect the upper ocean, including sub-mesoscale upwelling and downwelling, internal waves, storm surges, and tides. Atmosphere-only models that lack ocean and wave coupling cannot realistically represent the energy transfer and interactions between the atmosphere and the ocean and its waves. As such, TC research and prediction increasingly employed coupled atmosphere–wave–ocean modeling in the late 2000s (Chen *et al.*, 2007; Warner *et al.*, 2010; Liu *et al.*, 2011; and Zhang *et al.*, 2009a). These modeling systems, which remain among the state-of-the-art tools called upon today (e.g., Wu *et al.*, 2019), are composed of independently developed atmosphere general circulation, ocean general circulation, and phase-averaged spectral wave model components (Pringle and Kotamarthi, 2021). Given the significance of surface gravity waves in both global- and regional-scale modeling, Secs. III B 1 and III B 2 provide a comprehensive review of the direct and indirect impacts of waves on TC prediction; Sec. III B 3 reviews the most well-validated, fully coupled atmosphere–ocean–wave models; Sec. III B 4 reviews the impacts of spatial resolution in regional-scale models on major tropical cyclones.

1. Direct effects of waves through wave–atmosphere interaction

Waves characterize the surface roughness (z_0) of the ocean and are important for modeling winds above it. Without coupling between the atmosphere and waves, z_0 or the drag coefficient, C_d, are calculated as a function of wind speed alone (Charnock, 1955; Large and Pond, 1981; and Andreas *et al.*, 2012). When coupled with ocean wave models, z_0 can instead be computed using information directly inferred from the waves. Various formulations (Pringle and Kotamarthi, 2021) have been proposed to compute z_0, using wave steepness (Taylor and Yelland, 2001), wave age (Drennan *et al.*, 2005; Oost *et al.*, 2002), or two-dimensional wave spectra-dependent (Janssen 1989; Wu *et al.*, 2019). Some formulas to calculate z_0 are shown in Table I in the Appendix. For instance, in the Coupled Ocean–Atmosphere–Wave–Sediment Transport (COAWST) Modeling System (Warner *et al.*, 2010), the Taylor and Yelland formulation (Taylor and Yelland, 2001) was shown to enhance surface roughness, reducing the strength of the TC compared to experiments when the surface roughness is only calculated as a function of wind (Charnock, 1955). Furthermore, Zambon *et al.* (2021) compared the wave steepness and wave-age-based formulations and showed that the wave-age-based formulation in Oost *et al.* (2002) worked best for a Hurricane Florence (2017) hindcast, while Prakash *et al.* (2019) demonstrated that the wave-age-based formulation in Drennan *et al.* (2005) worked best for TC Vardah (2016). Another investigation of Hurricane Ida (2009) by Olabarrieta *et al.* (2012) also demonstrated that the predicted TC intensity and strength are considerably influenced by sea surface roughness parameterizations. Although surface roughness is associated with wave form, at very high wind speeds (>30 m s^{-1} at 10 m), surface roughness has been shown to saturate out due to spray generation and/or the flattening of wave crests (Donelan, 2004; Sullivan and McWilliams, 2010). In this case, the surface roughness (z_0) or drag coefficient (C_d) does not continue to increase with wind speed at high winds, and an upper limit to z_0 or C_d is often applied. These empirical parameterization methods are easy to be implemented in regional-scale models. However, since they are based on limited measured data, they cannot represent all the complex wind and wave conditions, especially during strong TCs. Therefore, wave boundary layer models (WBLM) that directly calculate the momentum transfer between winds and waves and currents within the wave boundary layer are also used (e.g., Janssen, 1991; Moon *et al.*, 2004; Reichl *et al.*, 2014; Chen and Yu, 2017; Du *et al.*, 2017; Larsén *et al.*, 2019; and Du *et al.*, 2022). Using WBLM, Moon *et al.* (2004) showed that while the drag coefficient increases with wind speed at lower wind speeds, this increase significantly slows down at higher wind speeds, eventually leveling off or even decreasing in some situations. In addition, the drag coefficient has a greater sea state dependence for fast-moving TCs compared to slow-moving storms or simple fetch-limited seas (Reichl *et al.*, 2014). To capture the decreasing tendency of the wind stress coefficient under storm conditions, Chen and Yu, 2016 incorporated the energy dissipation due to the stratification of sea spray into the WBLM. Du *et al.* (2017) further improved the WBLM by using it as a wind-input source function for the wave model, ensuring that the wave growth within the WBLM is consistent with the wave growth in the wave model. Chen *et al.*, 2013 and Chen and Curcic, 2016 developed a directional wind–wave coupling method to include effects of directionality of the wind and waves in hurricanes. This coupling approach considers short-wave spectral tails that produce surface stress and affect storm structure and intensity but are unresolved in most other wave models.

Another direct effect of waves on the atmosphere is that wave-breaking-induced sea spray may influence TC characteristics through changing momentum, heat, and moisture fluxes (Fairall *et al.*, 1994; Lighthill, 1999; Makin, 2005; Andreas *et al.*, 2015; and Prakash *et al.*, 2019). The relative importance of sea spray for predicting the TCs is still debatable. For example, Perrie *et al.* (2004, 2005) argued that sea spray can enhance the air–sea heat fluxes, which moderately increased the strength of the extratropical Hurricane Gustav in 2002 based on a coupled ocean–atmosphere–sea spray model (Andreas, 2003). Richter and Stern (2014) calculated the surface fluxes of enthalpy based on more than 2000 dropsonde profiles, and using the Monin–Obukhov similarity theory, indicated that the surface enthalpy fluxes are dominated by sea spray within TCs. However, Prakash *et al.* (2019) showed that the incorporation of sea spray flux has only a marginal influence on the intensity of a moderate cyclone. Sea spray can also indirectly influence the precipitation and intensity of tropical cyclones through sea salt aerosols (Hoarau *et al.*, 2018; Zhao *et al.*, 2022).

2. Indirect effects of waves through wave–current interaction

Waves can also influence the bottom boundary condition for TCs indirectly through wave–current interaction, which affects surface currents (Smith, 2006; Lane *et al.*, 2007; Olabarrieta *et al.*, 2010; and Mellor, 2016) and the SST through radiation stress, stokes drift, and wave-induced vertical mixing. Wave-induced mixing is the strongest effect compared to wave-induced roughness and Stokes–Coriolis drift on SST (Breivik *et al.*, 2015). Wave-induced mixing is primarily caused by wave breaking and wave orbital motion (Sullivan and McWilliams, 2010; Qiao *et al.*, 2004; and Babanin, 2006). Wave breaking-induced mixing occurs near the sea surface (Terray *et al.*, 1996; Toba and Kawamura, 1996) and typically has a limited impact on SST, heat fluxes near the surface (Zhang *et al.*, 2007; Craig and Banner, 1994; D'Alessio *et al.*, 1998; and Burchard, 2001), and the intensity and size of TCs. Wave orbital motion-induced mixing (also called non-breaking-wave-induced mixing), on the other hand, penetrates much deeper than wave breaking-induced mixing (Chen *et al.*, 2007; Qiao *et al.*, 2004; Babanin, 2006) and could reduce SST by bringing cold water upward through enhanced vertical mixing and mixed-layer depth, thus reducing TC intensification (Bruneau *et al.*, 2018; Li *et al.*, 2014; Zhao *et al.*, 2017; Zhang *et al.*, 2022). Without considering wave-induced mixing in ocean models, the SST and hence TC intensity can be overestimated (Qiao *et al.*, 2004; Kantha and Clayson, 1994; Martin, 1985; Babanin and Haus, 2009; Pleskachevsky *et al.*, 2011; Toffoli *et al.*, 2012; and Aijaz *et al.*, 2017). Indeed, Zhang *et al.* (2022) demonstrated that the wave-breaking-induced turbulence is negligible compared to wave orbital motion-induced mixing, although for some shallow mixed-layer conditions, the effects of wave-breaking-induced mixing might be also significant (Mellor and Blumberg, 2004; Sun *et al.*, 2005; and Huang *et al.*, 2011). The turbulence driven by wave orbital motion can be described using the one-dimensional formula in Ghantous and Babanin (2014) and included in two-equation turbulence closure schemes such as the Generalized Length-Scale (Umlauf and Burchard, 2003). The wave orbital motion-induced mixing is implemented into turbulence models by modifying the vertical viscosity or turbulent kinetic energy (TKE) source term (Song *et al.*, 2012; Qiao *et al.*, 2004; Wang *et al.*, 2010; and Babanin, 2011). With a coupled hurricane–ocean–wave modeling system, Aijaz *et al.* (2017) found that the non-breaking wave parameterization has different impacts on the weak and the strong sides of the storm track.

3. Regional-scale atmosphere–ocean–wave models applied to simulate TCs

The COAWST modeling system (Warner *et al.*, 2010) is widely recognized as a leading coupled modeling system. It integrates the Advanced Research Weather Research and Forecasting (WRF) model (Skamarock *et al.*, 2005; Powers *et al.*, 2017) for atmospheric dynamics, the Regional Ocean Modeling system (ROMS) (Shchepetkin and McWilliams, 2005; Shchepetkin and McWilliams, 2009; and Haidvogel *et al.*, 2008) for ocean circulation, the Simulating WAves Nearshore (SWAN) (Booij *et al.*, 1999) spectral wave model for nearshore wave simulation, and the Community Sediment Transport Modeling System (Warner *et al.*, 2008) for sediment transport studies. The SWAN model can be replaced with WAVEWATCH III (WW3) with similar capabilities (Pringle and Kotamarthi, 2021). These models communicate and share data through the Modeling Coupling Toolkit (MCT) (Jacob *et al.*, 2005; Larson *et al.*, 2005). Another significant coupled model is the First Institute of Oceanography Atmosphere-Ocean-Wave (FIO-AOW) (Zhao *et al.*, 2017) system. This model integrates WRF for atmospheric simulation, the Princeton Ocean Model (POM) (Blumberg and Mellor, 1987) for ocean dynamics, and the third-generation Marine Sciences and Numerical Modeling (MASNUM) wave model (Yuan *et al.*, 1991; Yuan *et al.*, 1992) through the Community Coupler version 1 (C-Coupler1) (Liu *et al.*, 2014). Additionally, several models have been developed based on the Nucleus for European Modeling of the Ocean (NEMO) (Madec and NEMO Team, 2016) for ocean circulation. Notable examples include the Chemical Hydrological Atmospheric Ocean wave System (CHAOS) (Varlas *et al.*, 2020), the Uppsala University Coupled model (UU-CM) (Wu *et al.*, 2019), and IFS-NEMO-Wave Model (WAM) (Breivik *et al.*, 2015). CHAOS couples the WRF model for atmosphere and the ocean WAM cycle 4.5.4 (WAMDI Group, 1998) for waves through the OASIS3-MCT version 3.0 coupler (Valcke *et al.*, 2015; Craig *et al.*, 2017). IFS-NEMO-WAM coupled the global numerical weather prediction model, IFS of the ECMWF, to model the atmosphere. In contrast, UU-CM utilizes WW3 for wave simulations and considers more processes such as the feedback of ocean/ice-induced water level changes on waves and the impact of waves on oceanic and ice dynamics, including surface Stokes drift, wave-supported stress, and the transfer of momentum and TKE from waves to ocean currents. For detailed descriptions of the coupling components, coupler used, and variables exchanged among different models, refer to Table II in the Appendix.

4. Spatial resolution impacts

Similar to Earth system models (Sec. III A), grid spacing in regional models continues to attain smaller scales as computational resources increase in time. Improvements in the representation of inner-core dynamical processes are a multi-scale problem, as the TC inner core interacts with the larger-scale environment (Wang and Wu, 2004; Davis *et al.*, 2008). Resolving the inner core of a TC with a grid spacing of less than 4 km has allowed the explicit representation of convection, which has resulted in a better depiction of TC structure (Fowle and Roebber, 2003). Gopalakrishnan *et al.* (2012) demonstrated improvements in TC intensity forecasts by decreasing nested grid spacing from 9 to 3 km using HWRF. In the COAWST modeling framework, the atmospheric WRF model also allows for a moving nested domain following the hurricane center. This, in turn, allows for continuous higher resolution of the TC inner core (Olabarrieta *et al.*, 2012).

C. Microscale models

Whereas Secs. III A and III B focus on global- and regional-scale modeling capabilities for TCs and ETCs, in order to design hurricane-resilient wind energy systems, the structure of the microscale turbulence within a hurricane and at the turbine scale must be better understood. Currently, there are only limited microscale turbulence data available from TCs and ETCs at heights relevant to modern turbines, which reach altitudes from 50 m to 300 m (He *et al.*, 2022). This is because surface-based measurement stations/devices or meteorological towers often incur damage during hurricane passage. Dropsonde data, on the other hand, are coarser in resolution and suffer from the inability to take longer-duration point measurements at a fixed location (as the wind turbine would experience the winds). Therefore, resorting to turbulence-resolving microscale simulations, namely, large-eddy simulation (LES), of the hurricane boundary layer is becoming increasingly important.

The structure of microscale turbulence in a hurricane boundary layer is an active field of research (Zhang *et al.*, 2009b; Montgomery and Smith, 2017; Huang *et al.*, 2018). Sub-kilometer-scale features of hurricane wind fields such as the organized turbulence structures of meso-vortices can create significant and unforeseen loads on OWTs. Similarly, roll vortices, a series of large-scale turbulent eddies that align along the mean wind and exhibit wavelengths varying from 200 to over 3000 m, have been found to exhibit strong fluxes that can change the hurricane structure and damage OWTs through intense surface winds. Although these roll vortices can be observed in the field using measurements from SAR (Huang *et al.*, 2018; Foster, 2005), Doppler weather radar (Gall *et al.*, 1998), and aircraft data (Tang *et al.*, 2021), many of their characteristics are extremely difficult to measure during actual storms because they occur in or near the eyewall of the hurricane where wind speeds are extremely high, and observations are difficult to make. Moreover, observations of the distribution and lifetime of these meso-vortices may also require simultaneous measurement of wind speed and direction over spatial domains measured in the tens of kilometers. LES thus has been employed to resolve the most important scales of flow and approximate other smaller scales of turbulence.

Examples of work on idealized hurricane LES include that of Rotunno *et al.* (2009), Ito *et al.* (2017), Li and Pu (2023), Li *et al.* (2021), and Ren *et al.* (2020, 2022). The work of Rotunno *et al.* (2009) is one of the earliest LES studies of a hurricane using idealized WRF with inner LES nests to better understand horizontal turbulent diffusion in hurricanes, which can then inform the turbulence model in mesoscale models used to simulate hurricanes. They show that a grid of roughly 100-m horizontal resolution is required to even begin to adequately resolve turbulence. By resolving turbulence, the mean intensity of the storm is decreased, but peak gusts are increased compared to results from mesoscale simulations in which turbulence is completely parameterized. It is noteworthy that hurricanes are mesoscale processes, so their horizontal extent is in the hundreds of kilometers, meaning hurricane LES at 100-m grid spacing can be extremely costly, and some sort of grid nesting is required to keep the cost tractable, especially when there is a desire to push to even finer resolution.

Li and Pu (2023) and Li *et al.* (2021) used WRF-LES data of the landfall of Hurricane Harvey to examine and try to understand the mechanisms for roll vortices in hurricane boundary layers. Their simulation shows extremely intense, organized roll vortices in the layer between 200 and 3000 m above the surface and 20–40 km from the hurricane center, roughly aligned with the mean flow and spiraling toward the core of the hurricane. They examine correlations between roll strength and Richardson number, shear, inflow convergence, and pressure perturbations throughout the storm. Ito *et al.* (2017) performed additional work to characterize coherent roll structures through idealized hurricane LES. Their work is somewhat different in that they use a different code, the Japan Meteorological Agency Non-Hydrostatic Model, and they characterize rolls in different ways than Li and Pu (2023), so the two works complement each other.

Although there are many more non-wind-energy LES studies meant to better characterize hurricanes and their turbulence (e.g., Stern *et al.*, 2016; 2021), here we focus on wind-energy-specific idealized hurricane LES research, including that of Worsnop *et al.* (2017a, 2017b), and Sanchez Gomez *et al.* (2023)—all of which have helped identify important wind turbine load drivers such as gust factors, spatial coherence, velocity spectrum, shear profile, direction change, and veer. With the inner $80 \times 80\,\text{km}^2$ region of their domain using Cloud model1, Worsnop *et al.* (2017a) showed that a Category-5 hurricane simulation compares well with Hurricane Isabel in terms of mean wind speeds, wind speed variances, and power spectra. Using the same hurricane simulations (Worsnop *et al.*, 2017a), Worsnop *et al.* (2017b) demonstrated that near the eye wall, 3 s gusts can exceed 100 m s^{-1} with 10-min mean wind speeds exceeding 90 m s^{-1}, agreeing with analysis of dropsonde wind speeds (Stern *et al.*, 2016). These values exceed the IEC standard T-turbine design standards and would cause extreme aerodynamic and structural loading that could lead to damage or failure. Gust factors can reach 1.7 in the eyewall, larger than the factor commonly used (1.4). Wind direction can shift by $10°–30°$ in less than 10 min, which has implications on whether wind turbine yaw systems react fast enough to keep the wind turbine oriented for minimal damage. Finally, Worsnop *et al.* (2017b) used the LES data to show that significant wind veer across the rotor disk is possible in the hurricane boundary layer and recommend that load simulations take the wind veer into account. Furthermore, Sanchez Gomez *et al.* (2023) recently conducted LESs on five hurricanes, ranging from Category 1 to 3, to study the hurricane boundary layer and its impacts on wind turbines. The simulations were performed using a five-domain WRF set up in which the inner two nests are LES. The SST is different in each of the five cases, ranging from 26 to 34 °C. Increasing the surface temperature causes both the near-surface wind speeds and the hurricane eyewall radius to increase. Sanchez Gomez *et al.* (2023) showed that hub-height (90 m) wind gusts, which are defined using a 3-s time-window mean, rarely exceed the IEC 61400-3 design standards (Knutson *et al.*, 2007) for Class I (50 m s^{-1}) and Class T (57 m s^{-1}) wind turbines. However, the 10-min mean hub-height winds in Category 2 (and 3) hurricanes exceed the design standards for Class I turbines 85% (100%) of the time. Even for the Class T design standards, the simulated 10-min mean hub-height winds of a Category 3 storm often exceed the design standard, but this exceedance is less frequent than for the Class I standards. They also show that wind speed gusts are often higher near the eyewall of the Category 2 or 3 storms than accounted for in the design standards. Wind-speed vertical shear was found to be nearly twice that specified in the standards. The wind direction change only occasionally exceeds $\pm 8°$, which is a different conclusion than Worsnop *et al.* (2017a), who simulated a Category 5 hurricane and found wind direction change across the rotor layer can range between 15° and 50°.

The above-mentioned LES studies include the simulation of an entire hurricane. Most of these types of simulations use a mesoscale grid to simulate a realistic tropical cyclone. A microscale inner high-resolution region is nested within the mesoscale region, where the large-scale system can drive the smaller-scale turbulent and coherent eddies within the nested LES region. Although it is very realistic, this kind of modeling system is complex and computationally expensive. Bryan *et al.* (2017) recognized the need for a simpler LES method to simulate hurricane boundary layers that they term the "simple method." In essence, this technique uses a rectangular domain that represents a hurricane-like boundary layer over a relatively limited region centered over a user-specified radial distance from a tropical cyclone center. In particular, the method is designed to represent regions outside of the inner-core eyewall region (e.g., 40 km from the hurricane center and beyond). Thus, in this LES configuration, additional source terms are introduced to the momentum equations of laterally periodic atmospheric LES. These terms represent the large-scale bulk advection of momentum and centrifugal effects of the hurricane on the boundary layer. Compared to dropsonde data, this method captures the shape of the hurricane boundary layer vertical profiles of velocity and turbulent stresses quite well, but the method presently cannot portray the complex three-dimensional flow near the eyewall where there is significant vertical motion and horizontal heterogeneity. This "simple method" has been implemented in the National Renewable Energy Laboratory (NREL) Simulator fOr Wind Farm Applications and AMR-Wind codes. In addition, Ma and Sun (2021) used the method with an atmospheric boundary layer LES code to study the effects of hurricane boundary layer winds on electrical transmission lines. More recently, Chen *et al.* (2021) extended the "simple" method to also nudge potential temperature and moisture profiles toward specified values.

In summary, the microscale modeling of hurricane flows offers tremendous potential in better understanding hurricane boundary layer physics and depicting hurricane impacts on wind energy and beyond. Hurricane LES therefore should facilitate better understanding of hurricane-driven wind farm failures such as those outlined by Chen and Xu (2016). It can also be used to help inform wind turbine design standards, especially in the realm of turbulence modeling, gust modeling, and understanding of shear, veer, and wind direction changes. Ultimately, hurricane microscale modeling can provide a means to develop and test novel ideas in making hurricane-resilient wind energy systems.

IV. AI/ML-BASED DATA-DRIVEN MODELING STUDIES

Although the previously discussed numerical models can simulate complex physical processes in both the atmosphere and ocean during TC and ETCs, these models are computationally expensive and therefore limit the amount of data that can be created (i.e., hundreds of years' worth data) to accurately estimate risks from these storms. Fortunately, AI and ML methods are in the midst of a renaissance, finding innumerable applications in solving complex computational problems in a much more efficient way. For example, AI/ML methods have been used for exploring and extracting useful information from gigantic datasets, automating and streamlining painstaking processes, and proving adept at solving other difficult problems. Both private industry and the geosciences, and more specifically the TC research community, are adapting AI/ML technologies into many realms of research and forecasting at a breathtaking pace. As long appreciated in statistical modeling, AI/ML techniques do best when provided sufficiently voluminous training data or when combined into other algorithms that better constrain AI/ML models with empirical or known physical processes. In particular, AI/ML has proven useful in diagnosing a TC's intensity and wind structure from satellite data, and in predicting important aspects of TCs such as formation, storm track, intensity, wind structure, and even downstream applications such as TC-driven ocean waves. We provide an overview of some of the AI/ML successes in the TC diagnosis and prediction problems relevant to offshore wind farms in Sections IV A—IV E.

A. Pointwise downscaling of winds

In offshore wind farm applications, it is advantageous to have an accurate depiction of the winds experienced locally at a specific point or in a very small area (e.g., a wind farm or an area with few wind turbines) near the Earth's surface. As a close cousin of diagnosing and predicting wind structure, pointwise TC wind diagnosis and prediction is a relatively new area of study in TCs. Nonetheless, significant headway has been made recently. Overall, this application is a type of downscaling from a coarser spatial–temporal analysis or model prediction to fine-grained spatial–temporal scales relevant to wind turbines. One promising technique in pointwise probabilistic wind speed exceedance thresholds was developed by Lin *et al.* (2020). Here, a track model generating O(1000) synthetic tracks statistically consistent with numerical weather prediction (NWP) models and time varying environmental predictors is used in conjunction with an intensity model to predict intensity along each track. In addition, using a modified version of the physically based model of Chavas *et al.* (2015), a two-dimensional surface wind field is generated for each track member. This ensemble technique provides a detailed probabilistic outlook for pointwise winds. Another recently proposed approach to downscaling uses deep neural networks (DNNs), specifically DNN-based super-resolution (SR) techniques. In digital image processing, DNN-based SR (Dong *et al.*, 2014; Yang *et al.*, 2014) describes various algorithms that take one or more low-resolution images and generate an estimate of a high-resolution image of the same target (Tian and Ma, 2011), a concept closely related to downscaling in climate modeling. Another DNN variant, the generative adversarial network (GAN) (Goodfellow *et al.*, 2014), has been used to improve feature loss or realism of the super-resolution convolutional neural networks (CNNs) (Ledig *et al.*, 2017; Stengel *et al.*, 2020). SR-GAN was demonstrated to be able to capture the microscale turbulence characteristics in complex terrain (e.g., mountain and coastal) by Haupt *et al.* (2021) and Dettling *et al.* (2022). Most recently, diffusion models are being applied to develop SR models for wind downscaling at a few kilometers (e.g., Merizzi *et al.*, 2024; Kurinchi-Vendhan, 2023).

B. Intensity diagnosis and prediction

As discussed in the beginning of Sec. III, improving TC intensity prediction remains a top priority and a challenge at operational forecast centers worldwide. Moreover, given the lack of *in situ* observations over the oceans, using information from satellite data to accurately quantify the storm's intensity is highly prized. In both diagnosis and prediction, AI/ML is making beneficial strides. CNNs are particularly well suited for diagnosing intensity from satellite imagery because, provided sufficient training data, they can decipher relationships between spatial cloud patterns and storm intensity (Pradhan *et al.*, 2018; Wimmers *et al.*, 2019; Chen *et al.*, 2019; Lee *et al.*, 2020; Tan *et al.*, 2022; Gurung *et al.*, 2023, among others). In the prediction of intensity, a vast spectrum of AI/ML tools have been brought to bear on the problem, with analog ensembles (Alessandrini *et al.*, 2018; Lewis *et al.*, 2020), evolutionary programming (Schaffer *et al.*, 2020), feed-forward (FFNNs) (Cloud *et al.*, 2019); CNNs (Griffin *et al.*, 2022; Varalakshmi *et al.*, 2023), gradient boosted regression tree models (Zhu *et al.*, 2022), combined recurrent NN (RNN)/CNN architectures (Jiang *et al.*, 2022), and a consensus of methods (Chen *et al.*, 2023) showing promise in deterministic intensity prediction or probabilistic rapid intensification prediction. It is also likely DWP predictions will provide competitive or superior intensity predictions before long.

C. Wind structure diagnosis and prediction

Like intensity, accurately determining the horizontal, near-surface TC wind structure is highly constrained by the lack of *in situ* observations over the ocean. Empirical methods using satellite data so far have offered a propitious path toward inferring TC wind fields. Although regression techniques have long existed for estimating the wind field from satellite data, AI/ML techniques have accelerated improvements in regression. Lu *et al.* (2022) used support vector machine methods and general regression NNs. Xu *et al.* (2022) used both infrared (IR) and microwave satellite imagery with a CNN to estimate TC size. Zhuo and Tan (2021) found a deep CNN with auxiliary information about a TC's environment produces promising estimates of intensity, size, and structure from satellite data. Tian *et al.* (2023) expand upon these ideas and offer a framework for AI/ML-based size estimation from multiple satellite channels, where multiple AI/ML steps are applied. IR satellite data are ingested into four layers of two-dimensional convolutions. Simultaneously, a three-dimensional convolution is applied in four layers to multiple satellite channels. Spatial IR features and channel features are then sent into their own CNNs. In the final step, a multitask learning model is used to give both intensity and size estimates for the TC. This step includes additional information about the TC's environment. Baek *et al.* (2022) similarly found multitask methods to be successful in TC size estimation. Multistep methods like this are likely to produce lower errors than existing operational methods and recent simpler deep-learning approaches.

Outside of the realm of satellite estimates, a variety of AI/ML techniques have been adapted to estimate TC wind structure with other input data. To determine wind structure in some given real TCs, Snaiki and Wu (2019) combined deep learning with idealized Navier–Stokes equations to base AI/ML estimates of the TC boundary layer winds upon physical constraints and basic observational estimates of the state of the storm. Parametric wind structure methods may also be enhanced in future research using AI/ML (Yan and Zhang, 2022). Yang *et al.* (2022) recently developed a decision-tree-based algorithm to reconstruct detailed TC wind fields using HURDAT2 and ERA-Interim data. A key purpose of Yang *et al.* (2022)'s technique is to capture the azimuthally asymmetric wind structures that can arise from numerous factors, including storm motion, vertical wind shear, TC interactions with land, ETT, interactions with convective-generated vorticity anomalies inside the vortex, and other mesoscale-convective interactions. So far, there has been no significant progress in predicting 3D TC wind fields with AI/ML, but methods used for other TC prediction problems should be adaptable to wind field prediction. For example, AI/ML may be used to post-process NWP or DWP output to improve predictions of TC wind fields. Moreover, given the pace of advancements, DWP models for direct regional mesoscale simulation will likely evolve with more reliable 3D wind structures for TCs in the near future.

D. Track prediction

TC track predictions are important in determining when to shut down wind turbines and they can also provide historical data in which to conduct model validation. Most of the research using AI/ML in track prediction falls into the category of observational data fusion problems (Giffard-Roisin *et al.*, 2020) and/or NWP post-processing. However, it is possible to create a skillful model simply using the observational HURDAT2 dataset of TC tracks to train a recurrent neural network (RNN), specifically an LSTM version to contend with a so-called "vanishing gradient problem" (Bose *et al.*, 2022). Most track prediction methods benefit from fusing multiple sources of observational and predictive data to generate a satisfactory track forecast. Hybrid neural network techniques to deal with multiple types of input data offer a potentially optimal path for TC applications including track prediction. For example, Cheung *et al.* (2022) used a CNN to extract spatial patterns in Global Ensemble Forecast System (GEFS) output, a FFNN for GEFS-predicted TC positions, and an LSTM RNN to capture information from previous time steps. This post-processing technique improves upon the skill of the GEFS track forecasts. Kumar *et al.* (2023) also found success in extended lead-time track prediction combining AI/ML methods. Other recent work in the area of track prediction includes the use of an RNN (Kordmahalleh *et al.*, 2016; Gao *et al.*, 2018; Alemany *et al.*, 2019), a genetic NN (Huang and Jin, 2013), and empirical ensemble methods (Dong and Zhang, 2016). Recently, researchers, many of whom work in private industry, have rapidly advanced Data-driven Weather Prediction (DWP) models using global reanalysis datasets (Pathak *et al.*, 2022; Chen *et al.*, 2023; Lam *et al.*, 2023; and Nguyen *et al.*, 2023). Many of these types of AI/ML models successfully produce extended range global weather predictions and even include the ability to produce excellent TC track predictions (Bi *et al.*, 2023).

E. Wave prediction

Extreme waves generated by tropical and extratropical storms pose a significant hazard to offshore wind energy infrastructure. Prediction models often depend on the wind fields diagnosed or predicted in applications alluded to above. Ocean waves are often simulated in physical models, but AI/ML is increasingly being incorporated into the general problem of determining significant wave heights. In the last 5 years, in fact, AI/ML-based studies have proliferated on this specific topic. For example, Minuzzi and Farina (2023) used a long short-term memory (LSTM) with ERA5 reanalysis and buoy data to forecast significant wave height. Song *et al.* (2022) combined both a CNN and LSTM and applied the methods to ERA5 reanalysis data to target physical model-simulated waves. Domala *et al.* (2022) more comprehensively discussed empirical methods for significant wave height prediction. These studies are often directed toward more typical sea states rather than the violent conditions imposed by extreme storms. Some AI/ML-based work has been conducted for TC-induced waves (Mafi and Amirinia, 2017; Chen, 2019; Meng *et al.*, 2021; Wei, 2021; and Bethel *et al.*, 2022) and other AI/ML tools have been used to understand offshore platform integrity in the midst of significant oceanic waves (Dyer *et al.*, 2021). Overall, more study is needed for the more extreme TC winds that create a very complex sea state, both at a basic research level and in AI/ML applications.

V. CLIMATE CHANGE IMPACTS ON TC AND ETC

Prior to the 19th century, aspects of TC activity have been inferred from paleotempestology (Rodysill *et al.*, 2020; Altman *et al.*, 2021; Mann *et al.*, 2009; Toomey *et al.*, 2013). From the 19th century to present, changes in TC activity are assessed using the best-track dataset, which relies on observations available at the time. Because TC observations greatly improved with the deployment of geostationary satellites in the 1970s, and satellites improved thereafter, a more reliable observational record extends from around 1980 to the present. Many historical studies have thus focused on this period. Chand *et al.* (2022), Klotzbach *et al.* (2022), and Emanuel (2021) noted an increasing number of storms in the North Atlantic using different methods. However, there has been no statistically significant change in the number of landfalling TCs (Vecchi *et al.*, 2021). From 1980 to 2020, there has been an increase in mean TC intensity (Kossin *et al.*, 2020; Emanuel, 2020; Elsner, 2020). There is also evidence of slower mean translation speed (Kossin, 2018), heavier precipitation (Touma *et al.*, 2019), and slower inland decay rates (Li and Chakraborty, 2020). Bhatia *et al.* (2019) found that TC intensification rates have increased in the North Atlantic.

To understand future changes in TC intensity and frequency under a changing climate, GCMs and ESMs are often used. In these models, the intensity and frequencies of TCs are very sensitive to horizontal grid spacing, because resolving the inner core is necessary to capture processes responsible for intensity variability, as already been discussed in Sec. III. Discrepancies among different climate model integrations also result from different forcings, feedback from aerosols, and clouds, among other factors. Most climate modeling studies show a global decrease in the number of TCs (Knutson *et al.*, 2020) in future climates under a projected 2 °C warming (median decrease in 14%), although a few studies show an increase (Emanuel, 2021). Projected TC frequencies in different basins are more variable. Additionally, most studies show frequency reductions in the Southern Hemisphere (Roberts *et al.*, 2020) while the Northern Hemisphere is more uncertain. Theory and climate modeling studies show that, globally, the strongest TCs are likely to get stronger in future climates, thereby increasing the fraction of intense TCs to total TCs (Knutson *et al.*, 2020), consistent with findings based on observational records (Kossin *et al.*, 2020). Notably, this trend is also evident in the North Atlantic basin (Chauvin *et al.*, 2020). One important, yet more unpredictable factor impacting TC activity on climate and seasonal timescales is Saharan-born dust. Strong *et al.* (2018) and Reed *et al.* (2019) found that increases in Saharan dust aerosols decrease TC activity in the North Atlantic basin.

Using the CMIP6 ESM output, Balaguru *et al.* (2023) noted that the Coastal Hurricane Frequency will increase over the Gulf Coast and lower East Coast with a maximum over the northern Gulf Coast and Florida. This was attributed to the strengthening of upper tropospheric circulation above the western Atlantic. The study (Balaguru *et al.*, 2023) also highlights the sensitivity of projected large-scale winds to tropical heating and precipitation changes, which are driven by the spatial pattern of future SST warming. The inter-model uncertainty of projected heating trends is constrained by the response of the equatorial Pacific zonal SST gradient to climate change. Liu (2014) developed a hurricane simulation program based on Vickery *et al.* (2000) to assess the impacts of two climate change effects (change in annual storm frequency and sea surface temperature) on future U.S. design wind speeds for the coastal regions and projects potential hurricane losses under different speculated future climate scenarios. Results show potential increases of losses of buidlings in the Gulf Coast of up to 46% by the end of the century, highlighting the significant increase in hurricane risk for coastal regions due to climate change. Emanuel (2021) applied a downscaling technique described in Emanuel *et al.* (2006, 2008) to study the impact of anthropogenic climate change using CMIP6 models. The study found an increase in probability of rapid intensification. The study also found an increase in storms stalling, which can cause extensive damage due to rainfall and winds.

Given the future projections of TC changes from various Earth System models, NOAA released a fact sheet in 2023 quantifying expected impacts of climate change on hurricanes by the end of the 21st century in the North Atlantic basin (NOAA, 2023). A 2 °C increase in global mean temperature is expected to result in the following: storm inundation rise of 2–3 ft, rainfall rate increase in 15%, 10% increase in Category 4–5 hurricanes, 15% decrease in total storms, and projected increase in 3% in the strongest winds. Although studies have identified trends in the North Atlantic basin as a whole, there is less certainty about changes in activity in local parts of the basin, such as the continental shelf off the U.S. East Coast, where OWTs may be deployed.

Future projections of ETT of TCs are more complicated, because they are affected by both changes in TCs (e.g., frequency, intensity, and size) and changes in the midlatitude environment. Several previous studies suggest that warmer SSTs and reduced wind shear in the North Atlantic tropics and subtropics create a more favorable environment for TC survival. This will allow them to reach baroclinic zones more often in the future, resulting in an increase in the percentage of ETT events (Liu, 2014; Michaelis and Lackmann, 2019; and Michaelis and Lackmann, 2021). Haarsma *et al.* (2013) and Baatsen *et al.* (2015) showed similar results in their future climate simulations: a projected increase in TC intensity along with a poleward shift in TC genesis region. Studies that examined storm-scale ETT changes in response to climate change have observed lower minimum sea-level pressure (SLP) and stronger maximum sustained winds, along with significant increases in precipitation during the ETT and post-ETT phases of tropical storms in Representative Concentration Pathway 8.5 scenario by 2100 (Michaelis and Lackmann, 2019; Michaelis and Lackmann, 2021; Jung and Lackmann, 2019; Jung and Lackmann, 2021, and Jung and Lackmann, 2023). These studies portend an increased risk of coastal flooding and storm surges, including in higher latitudes such as the northeastern United States.

Finally, Kiran and Balaji (2022) used the COAWST framework and considered atmosphere and ocean coupling to study climate change impacts on two severe TCs in the Bay of Bengal. They use pseudo-global warming (PGW) methodology to project the cyclones to future (i.e., 2075) climatic conditions for RCP 4.5 and 8.5 scenarios.

They find that (1) compared to the current conditions, the maximum sustainable wind speed increases by 7.2 km h^{-1} for both cyclones for the RCP 8.5 scenario in 2075; (2) accumulated cyclone energy, power dissipation index, and precipitation were also projected to increase in future climatic conditions; (3) cyclones will intensify more in the future due to the combined effect of increased upper ocean heat content and reduced translation speed. However, this study (Kiran and Balaji, 2022) ignored the impacts of waves on the atmosphere and ocean component, which are important to realistically capture the TC intensity.

VI. RISK ASSESSMENT

OWT risk assessment is a critical aspect of the resilience and durability of OWT infrastructure (Staid *et al.*, 2015). Advanced computational models are used to simulate the complex interactions between hurricanes and OWTs, enabling engineers to evaluate the structural response, dynamic behavior, and potential failure modes under extreme wind and wave conditions (Kapoor *et al.*, 2020). In the current IEC 61400-3 (Knutson *et al.*, 2007) metocean design basis, 50-year extreme joint wind/wave conditions for ultimate loads and 500-year conditions for robustness checks are required. To date, most offshore wind has been established in the North Sea and other western European water bodies, which are mostly at risk from ETCs/European windstorms (Buchana and McSharry, 2019). The difficulty for the U.S. Atlantic and Gulf coasts, and to a lesser extent southern California, is that we move into a mixed climate featuring TCs, which are not present in western Europe. Research has shown that this mixed climate needs to be treated carefully, with separate extreme value distributions between TCs and ETCs (O'Grady *et al.*, 2022). At the 50-year level, depending on location, we could be close to the intersection of these extreme value distributions, meaning that either TCs or ETCs could be driving the ultimate design loads. On the other hand, the 500-year event for robustness check is certainly associated with a TC risk. In addition, the analysis needs to consider loads from a variety of factors including wind speeds (with turbulence intensities), wave heights and other hydrodynamic loads, rainfall, lightning, and their joint probabilities. The impact of climate change on tracks and intensities of TCs and other storms (see Sec. V) also need to be considered over and beyond the lifetime of the wind farm. The following subsections highlight risks to OWTs from ETCs and TCs.

A. ETC-driven wind and wave risks

ETCs are common offshore of the mid-Atlantic and northeast U.S. coastlines during the cool fall and winter seasons (Colle *et al.*, 2013), with similar occurrence frequencies to the North Sea and other western Europe water bodies (Ulbrich *et al.*, 2009). However, the strongest 5% of ETCs are more common in the northeastern U.S. and Gulf of Maine regions (5–10 cyclone days per cool season) than most of western Europe (1–5 cyclone days per cool season) (Ulbrich *et al.*, 2009). In the most extreme cases, near-surface wind speeds for ETCs can approach those of Category 1 hurricanes (Letson *et al.*, 2021; Pringle *et al.*, 2021). An analysis using ERA5 reanalysis for ETC-driven wind and wave risks offshore of the mid-Atlantic and northeastern U.S. coasts estimates that the 50-year event will have 30–40 m s^{-1} wind speeds at 100 m above sea level, and significant wave heights more than 15 m (Barthelmie *et al.*, 2021). Analysis in the North Sea shows that towers may buckle due to extreme extratropical windstorms, although there are relatively low annual probabilities, particularly for yawing turbines (Buchana and McSharry, 2019). Over a 20-year period at the Horns Rev II wind farm (91 turbines total), it was estimated by Buchana and McSharry (2019) that the 1% exceedance probability for buckling is 10 towers, with ~95% probability of no tower buckling occurring over that time period. Average annual losses for all North Sea wind farms are estimated at ~2M euros, and European union solvency requirements could require insurers hold 49M euros for payouts (computed from the 200-year event).

B. TC-driven wind and wave risks

Hurricanes generate extreme winds that may far exceed those of ETCs and current design standards, causing excessive damage to OWTs along Atlantic and Gulf coastal waters of the United States. Rose *et al.* (2012) were the first high-profile example to assess this risk based on historical hurricane statistics at selected locations. They found that hurricanes exceeding design limits caused buckling failures, with over half of the towers of a 50-turbine wind farm buckling during a Category 3–5 hurricane. In a Galveston, Texas, offshore wind farm, 32% of the towers would be expected to buckle over a 20-year period. Backup yaw power and the ability to yaw quickly with rapidly changing wind directions in hurricanes was identified as an important factor for reducing damage.

However, the limited historical record is generally considered inadequate for determining accurate statistics of Atlantic TCs, because it is relatively rare for them to pass over or near a particular offshore wind farm. To solve this problem, Emanuel *et al.* (2006) first developed a synthetic downscaling method for TCs that can be used to generate databases of events spanning 10 000–100 000 years or more, in order to better estimate return periods compared to the ~50 years of quality historical data since the satellite era. As described in Emanuel (2006), the method involves randomly drawing hurricane origins points from a genesis probability model (e.g., Poisson or negative binomial distribution of location-specific statistics), moving the hurricane according to environmental flows with a correction for beta drift (or using location-specific statistics of forward speed and direction), and applying an intensity model based on environmental variables such as the SST, atmospheric pressure, atmospheric temperature, ocean mixed-layer depth, and thermal stratification of the ocean below the mixed layer. Nowadays, several of these databases are available in the research community (Hallowell *et al.*, 2018; Lee *et al.*, 2018; Bloemendaal *et al.*, 2020; Bloemendaal *et al.*, 2022; and Balaguru *et al.*, 2023).

A notable study using such a synthetic TC database for hurricane risk assessment of OWT in the Atlantic basin came from Hallowell *et al.* (2018). Based on 100 000 years' worth of hurricane-induced wind and waves, they estimate that the mean lifetime (20-year) probability of structural failure for a tower or monopile of OWTs in U.S. Atlantic coast wind farms range between 7.3×10^{-10} and 3.4×10^{-4} for a functional yaw control system, and between 1.5×10^{-7} and 1.6×10^{-3} for a nonfunctional yaw control system. These estimates of failure are far lower than those of Rose *et al.* (2012). As an example, Hallowell *et al.* (2018) estimated an expected failure of 0.01 turbines for a 1223 OWT wind farm in New Jersey over a 20-year lifetime, while Rose *et al.* (2012) estimated that about 1 turbine would fail in a 50 OWT New Jersey wind farm; this is about three orders of magnitude different. Both studies use the NREL 5 MW offshore baseline turbine. Getting to the bottom of this large discrepancy would seem to be a high priority.

A key question is whether this discrepancy arises mostly from differences to damage fragility curves or from the hazard description. To give one hypothesis, Rose *et al.* (2012) potentially overestimated the wind speeds for the OWTs by only using the maximum wind speed, while Hallowell *et al.* (2018) used parametric hurricane models to describe the spatiotemporal variations of wind and wave fields for each synthetic TC event.

Recently, Balaguru *et al.* (2020, 2023) developed a RAFT using statistical and AI/ML approaches to generate synthetic hurricanes and provided insights to understand coastal hurricane risks as a result of climate change. Kim and Manuel (2016) formulated a framework for intensity evolution of TCs and utilized it to simulate wind patterns around wind farms. Their research assesses the risks posed to wind turbines by examining both the load distribution experienced and the probability distribution of wind speeds exceeding certain thresholds for each individual turbine.

C. Other hazards induced by TC and ETC and their impacts on OWTs

Although the duration of a TC or ETC event is much shorter than the lifespan of an OWT, OWTs can be vulnerable to certain hazards induced by these transient, yet extreme weather events. Reports indicate that a single catastrophic event can lead to severe damage to the structure and performance of OWTs, as reviewed below.

1. Rainfall

Siddons *et al.* (2015), Mishnaevsky *et al.* (2021), and Pryor *et al.* (2022), and others noted that leading-edge erosion (LEE) of wind turbine blades is a critical issue caused by raindrops, hailstones, and other particles. LEE not only reduces aerodynamic efficiency, but also accelerates premature failure, both of which impact the generation of power and lead to a reduction in annual turbine energy production. In recent years, specialized coatings and leading-edge tapes have been developed to act as sacrificial surfaces. As the size and blade diameter of wind turbines increase, the speed of the blade tips rises significantly. As a result, the impact of raindrops, hail, and other particles on the lifespan of these turbine blades has become more pronounced. Herring *et al.* (2020) analyzed measurements of offshore precipitation for a year using a disdrometer that was positioned 5.56 km offshore from the coast of Blyth, Northumberland. The dataset was compared to the most widely used droplet size distribution (Best, 1950), which often is used to represent onshore precipitation. Herring *et al.* (2020) found that this widely used distribution did not fit the offshore data and that any lifetime predictions made using this distribution are likely to be inaccurate. Such a shortcoming may result in a significant underestimation of the severity of the offshore conditions that cause LEE. Thus, improvements in the hydrometeor drop size distributions in marine TCs and ETCs are needed to accurately quantify hydrometeor impacts on turbine blades.

2. Lightning

Currently, operational and planned offshore wind plants are vulnerable to lightning strikes, as lightning tends to be more intense over the ocean than land, likely because the conductivity of the saline water is higher compared to moist soil (Asfur *et al.*, 2020). Turbine heights are increasing, adding to the risk of lightning strikes. Lightning strikes can cause severe damage to OWTs, especially to the blades (Garolera *et al.*, 2016; Hsu *et al.*, 2018). Tao *et al.* (2018) performed transient analysis using a complete circuit model for OWTs during lightning strikes to multiple blades. They found that the transient potential rise on OWTs and induced over-voltages at cable terminals could harm the facilities and equipment of the OWTs. Hence, more research needs to be conducted to combat lightning strikes for OWTs. Using 9 years of observation detection, Holzworth *et al.* (2019) found there are superbolts happening mostly over the water going right up to the coast. Superbolts are extremely rare, about a thousandth of a percent, and are most common in the Mediterranean Sea, in the northeast Atlantic Ocean, and over the Andes Mountains. There were just a few detected over the East Coast of the United States from 2010 to 2018, indicating the superbolt might be less of a concern compared to regular lightning strikes.

3. Tornadoes

The formation of TC-induced tornadoes is well documented in Edwards and Mosier (2022). There have been several reports of tornadoes damaging wind turbines, including breaking one or more blades (https://www.weather.gov/ind/). Lopez Ortiz (2023) simulated a tornado impacting a wind turbine and conducted sensitivity experiments with varying turbine locations, orientations, and operational conditions that may lead to structural failures or reduced loads. The study found that changing the yaw angle of the rotor plane and blade direction could reduce the load. These studies and findings are helpful for understanding the potential damage of tornadoes to OWTs. Waterspouts have the same characteristics as land tornadoes, and are associated with severe thunderstorms. They are often accompanied by high winds and waves, large hail, and frequent dangerous lightning.

4. Storm surge

Storm surges driven by TCs and ETCs could become important for offshore wind energy for those turbines located in relatively shallow depths, especially on wide continental shelves where surge is amplified (Resio and Westerink, 2008). In particular, strong currents near the seabed associated with storm surge and waves may cause scouring around the turbine foundations and buried submarine cables that transport power onshore (Gao *et al.*, 2024). There is also the danger of storm surge causing inundation of the substations located onshore or nearshore. Since substations are the most critical components of an offshore wind farm the inundation risk is important to consider.

VII. SCIENTIFIC GAPS AND RESEARCH NEEDS

After surveying the current landscape of observational capabilities, Earth system models, weather and regional-scale models, microscale models, and ML-based data-driven models focused on their applications in TC/ETC events relevant to offshore wind energy, we have established a foundation for understanding the strengths and potentials of these approaches. We explored the impacts of climate change on TCs and ETCs, as well as the associated risks posed by these phenomena. The primary goal of our review is to provide comprehensive information that enhances risk assessment practices and wind turbine resilience against TC and ETC threats. Despite considerable progress in these areas, there is still a substantial need for further technological development to accurately measure and simulate the extreme weather conditions caused by TCs and ETCs—such as high winds, significant wave heights, rapid wind direction changes, and intense turbulence. In light of this, the following sections outline the scientific gaps and future research needs identified from our thorough review of state-of-the-art methodologies. We propose a set of research priorities and directions for the community to collaboratively explore. These insights aim to not only spur further investigation but also serve as a foundation for refining wind turbine design and IEC design standards, thereby advancing our ability to mitigate risks associated with severe weather events.

A. Observations and validation

Although not all aspects of the TC are adequately sampled, certain parts have been observed better than others. Visible and infrared satellites sensors can observe the upper-level evolution of the cirrus cloud canopy; historically, the intensity of TC has been correlated with these patterns (i.e., the Dvorak technique). Microwave sensors on polar orbiting satellites have been used to map spatial patterns of ice particles and warm rain associated with the TC eyewall and spiral rain bands. Away from the dense cirrus canopy, atmospheric motion vectors (which track clouds and water vapor in successive satellite images) have been used to map the vertical structure of the winds near the TC. Some TCs have been reasonably well sampled at flight level during aircraft reconnaissance missions (3000 m above sea level). However, they are rarely thoroughly sampled in the boundary layer and near the surface, which is the primary area of interest for OWTs. Remote measurements such as Stepped-Frequency Microwave Radiometer, SAR, and Doppler radars help fill some of the gaps in this region, but more *in situ* observations are sorely needed. Due to extreme winds, crewed aircrafts typically cannot enter these regions; therefore, sampling must be done by UASs or remotely by satellites (e.g., SAR). Near-surface turbulence and characteristics of the air–sea interface have generally not been very well observed, particularly in intense TCs, although new platforms such as saildrones, balloons, and UASs show tremendous promise in obtaining larger quantities of valuable data in this region. Finally, data sharing between public and private sectors is important for enhancing collaboration and better informing decision-making in terms of risk resilience (Wang *et al.*, 2024).

B. Numerical and AI/ML-based modeling

1. Earth system modeling

Including wave processes in ESMs presents significant computational and scientific challenges, from the high resolution required to accurately simulate these interactions to the evolving understanding of waves' impacts on the climate system. Advances in computing power and modeling techniques, however, are gradually enabling the integration of these complex processes, enhancing the models' accuracy and predictive capabilities. For example, FIO-ESM v2.0 employed a wave model that includes the effect of surface wave Stokes drifts on air–sea momentum and heat fluxes as well as the effect of wave-induced sea spray on air–sea heat fluxes (Bao *et al.*, 2020). The U.S. Department of Energy's (DOE's) E3SM Project team has coupled WW3 into E3SM (Ikuyajolu *et al.*, 2023; Brus *et al.*, 2021). The coupling alters the atmospheric wind stress based on the Janssen's (1991) modified Charnock parameter (Charnock, 1955) that takes into account the wave stresses. On the ocean side, momentum fluxes are calculated by subtracting the total wave stress from the atmosphere momentum flux to account for a sea state not in equilibrium with the winds due to the growth and dissipation of the wave field (Ikuyajolu *et al.*, 2024). Studies are being conducted to evaluate the impacts of the wave coupling on climate at seasonal and subseasonal variabilities such as those that accompany the MJO (Ikuyajolu *et al.*, 2024). More comprehensive model validations are needed to understand the impacts of wave coupling on TC and ETC characteristics. Whereas many different modeling centers currently issue subseasonal and seasonal forecasts, the skill of these forecasts depends on the skill of simulating the MJO, QBWO, RWB, and ENSO as they are the dominant drivers of global TCs and ETCs (Sec. III A). The MJO has been simulated better in recent years with improvements to numerical weather prediction models (Vitart *et al.*, 2017). Overall, the ESMs do not exhibit skill beyond a seasonally varying climatology. To further improve the model performance, more efforts are needed for better representing the physical processes such as the interactions between the atmosphere, waves, and ocean. Additionally, improvements in spatial resolution, including the use of regional refined mesh (RRM) as seen in the E3SM, are essential. Studies have consistently indicated that a minimum spatial resolution of $\sim$25 km is required to capture the climatology of TC intensities, though it is still not sufficient to simulate major hurricanes of Category 3 and above. Thus, convection-permitting scale is crucial for ESMs to capture not only the large-scale seasonal and subseasonal variabilities but also the regional-scale characteristics of extreme weather events, including TC and ETCs on a sub-daily basis. Enhancements in the Simple Convection-Permitting E3SM Atmosphere Model (SCREAM) have been enabled by leveraging heterogeneous architectures found in DOE leadership computing facilities, along with the increasing computing power of general-purpose graphics processing units (GPUs). By integrating the simulation of oceans and waves with other critical components of the Earth's system into SCREAM across both climatic and weather time scales, the model's ability to accurately simulate extreme weather events will be significantly improved, which is crucial for addressing the challenges we face in predicting and understanding extreme weather impacts on wind energy.

2. Regional-scale modeling

At regional scales, developing the coupling between the atmosphere and ocean requires comprehensive knowledge about the ocean model. For example, establishing the correct open ocean boundary conditions is crucial yet challenging. These conditions significantly impact the simulation results, as they must accurately enable the exchange of heat, moisture, and momentum, and information between the model domain and the surrounding larger-scale environment. Furthermore, although interactions between the atmosphere, ocean, and waves have been considered in a limited number of models, the effects, especially from non-breaking waves, are not fully captured. For instance, phenomena such as non-breaking-wave-induced mixing and breaking-wave-induced sea spray are either overlooked or not well considered in most widely used fully coupled models (see the Appendix). Similarly, the concept of wave-induced surface roughness remains not fully understood, with various formulas available to parameterize it. However, these formulas yield different performances under various TC conditions.

The spatial resolution impacts from atmosphere, ocean, and wave models are significant as reviewed in Secs. III A and III B. The use of an unstructured grid, which provides ideal geometric fitting and flexibility for local topography refinement, has quickly gained popularity in research and applications to estuaries, coastal oceans, and the Great Lakes. This model framework allows for a high-resolution mesh over regions of interest, such as offshore wind plants, offering improved simulations of wind, wave, and current conditions. These enhancements are particularly necessary for mesoscale-to-microscale coupling, as reviewed in Sec. III C. However, most fully coupled regional or mesoscale models employ a regular grid for the ocean model, which does not allow regional refinement over regions of interest.

Achieving this additional high resolution over a region of interest poses a challenge, as it requires much shorter time steps, significantly increasing computational demands. GPU-accelerated version of these numerical models is desirable to simulate sufficient hurricane events for estimating risks, such as N-year return levels, at wind farms. Notably, no studies have employed fully coupled models in real hurricanes to assess their impacts on wind turbine design standards, including wind shear and veer, and to compare these against state-of-the-art observations, including dropsondes and sail drones. Finally, to study the impacts of global warming on TCs and ETCs, unlike the atmosphere-only model where only the PGW signal is needed for the atmospheric profiles, fully coupled atmosphere-ocean-wave models must also consider the PGW signal in the ocean component. Additionally, it is necessary to evaluate whether the PGW should account for only the thermodynamic changes (e.g., air temperature; Marciano *et al.*, 2015) or both dynamic and thermodynamic changes (e.g., air temperature, winds, and geopotential; Liu *et al.*, 2017), considering that winds are a crucial input for the wave models.

3. Microscale modeling and mesoscale-to-microscale downscaling

Although the simple method proposed by Bryan *et al.* (2017) is useful for downscaling the hurricane winds at a turbine scale, a major limitation of this method is that it assumes a laterally periodic domain, the simulation must be far enough from the storm center (20 km or so) so that radial gradients in the flow are small enough that the flow appears horizontally homogeneous across the LES domain. Furthermore, near the eye and eyewall, there is significant mean vertical motion of the flow, which cannot be captured by this method. Another limitation is that Bryan *et al.* (2017) presents this method such that the source terms do not vary with time. The equations for the source terms can also be made time varying to allow the domain to capture the effect of the translating storm. One can imagine this being of great value if simulating a day long wind farm simulation with actuator disks as the hurricane passes by the farm.

At the other end of the simplicity spectrum, we envision a domain with mixed inflow/outflow boundaries on all sides (except the bottom). The microscale lateral and upper domain boundaries can be provided by the mesoscale hurricane simulations on surfaces, such as velocity, temperature, and possibly moisture and turbulent kinetic energy. Additionally, the microscale domain lower boundary can be provided by mesoscale simulated heat flux, momentum flux, and sea surface temperature. These data are extracted at a certain frequency lower than the microscale time step, possibly as low as every 30 min. Additionally, some measure of the mesoscale background driving pressure gradient along a vertical column through the microscale domain is required. The data are interpolated in time and space to the resolution of the microscale simulation. The extracted background driving pressure gradient is applied as a time-height varying source term.

Last but not least, there appears to be potential in finding ways to drive hurricane microscale simulations not only with mesoscale simulations, but also with real field data. As the types of field data available increase over time (e.g., now we not only have dropsondes, but piloted gliders dropped from manned aircraft), and the quality of those data becomes better while computing power increases with the advent of exascale computing, the potential to fuse real and simulated data is exciting. In addition, the work about microscale hurricane modeling (described in Sec. III C) focuses on the atmosphere, but there is a need to better integrate wave/current effects into hurricane microscale simulations. We see this as a major area of research that holds potential to produce more realistic simulations. When considering wind energy, it is critical to faithfully capture not only the atmosphere and its turbulence, but also the waves and current, to understand loads on OWTs subject to hurricanes.

4. AI/ML-based modeling

Empirical dynamical methods have been successful in the frameworks of TC and weather prediction. In these approaches, physical principles are sagaciously integrated with statistical methods. Similarly, AI/ML methods often lack the beneficial integration of physical constraints that can help guide a method to successful solutions in research and prediction. Integrating physical constraints into AI/ML tools will benefit track, intensity, structure, wave, boundary layer modeling, and many other important applications in TC research and prediction. In the context of offshore wind turbines impacted by TCs, AI/ML advancements specifically in emulating LES simulations or high-resolution observations of TC boundary layers are needed in the near future. These efforts may be advanced through pure DWP methods or through downscaling from NWP predictions or reanalysis data. For all AI/ML applications, it is important to point out that the performance potential of AI/ML applications is far too often restricted by limited training data. In the age of AI/ML, calibrated and frequently updated datasets of both observational reanalysis data and NWP model output (e.g., several years of reforecasts from a TC NWP model using a frozen model configuration) should be curated or facilitated by funding agencies to allow AI/ML to reach its highest potential. In addition, operational AI/ML techniques must be flexible so that they can be readily tuned to new data or updated NWP model configurations. Too frequently, there are inadequate resources in operational centers to upgrade existing AI/ML methods once operational implementation is completed. Last, AI/ML techniques are frequently used as black box tools and the understanding of the physical reasons for certain predictions is often opaque. Physically interpretable AI/ML techniques need to become more of a standard practice to improve scientific and predictive insight.

C. Risk assessment and climate change

Currently, the offshore wind energy industry bases its return level estimates solely on historical data. For instance, synthetic hurricanes spanning tens and hundreds of thousands of years are generated using

TABLE I. Formulas for wave-induced roughness (z0), where u* is the friction velocity, HS is the significant wave height, Lp is wavelength at the peak of the wave spectrum, cp is the wave phase speed at the peak of the spectrum, and θ is difference of the wind direction and the peak wave direction (in radians).

References	Formula	Wave parameters
Taylor and Yelland (2001)	$Z_0/H_s = 1200 * \left(\frac{H_s}{L_p}\right)^{4.5}$ H_s is significant wave height, L_p is peak wavelength	Wave steepness
Drennan *et al.* (2003; 2005)	$Z_0/H_s = 3.35 * \left(\frac{u_*}{c_p}\right)^{3.4}$ u_* is the friction velocity, c_p is the wave phase speed at the peak of the spectrum	Wave age
Oost *et al.* (2002)	$Z_0/H_s = \left(\frac{25}{\pi}\right) * \left(\frac{L_p}{H_s}\right) * \left(\frac{u_*}{c_p}\right)^{4.5}$	Wave age, and wave steepness
Porchetta *et al.* (2019; 2021)	$Z_0/H_s = 20 * \cos(0.45\theta) * \left(\frac{u_*}{c_p}\right)^{3.8*\cos(-0.32\theta)}$ θ is the difference of the wind direction and the peak wave direction (in radians)	Wave age, and wave direction

TABLE II. Three well-validated, fully coupled ocean–atmosphere–wave models: COAWST, FIO-AOW, and UU-CM.

	COAWST (Warner *et al.*, 2010)	FIO-AOW (Zhao *et al.*, 2017)	UU-CM (Wu *et al.*, 2019)
Institute	Woods Hole Coastal and Marine Science Center, U.S. Geological Survey	FIO, Ministry of Natural Resources of China	The Uppsala University
Atmosphere model	WRF	WRF	WRF
Ocean model	ROMS	POM	NEMO
Wave model	SWAN	MASNUM	WW3
Coupler	MCT	C-Coupler v1	OASIS3-MCT
Variables exchanged between the atmosphere and ocean	WRF to ROMS: near-surface winds, relative humidity and air temperature, atmospheric pressure, cloud fraction, precipitation, shortwave and longwave net heat fluxes	WRF to POM: latent and sensible heat flux, friction velocity, sea spray latent and sensible heat flux, shortwave and longwave radiation flux	WRF to NEMO: atmospheric wind stress, downwelling and upward shortwave and longwave radiation, net water flux
	ROMS to WRF: SST	ROMS to WRF: SST	NEMO to WRF: surface current velocity, SST
Variables exchanged between the atmosphere and wave	WRF to SWAN: near-surface winds	WRF to MASNUM: near-surface winds	WRF to WW3: near-surface winds.
	SWAN to WRF: significant wave height, and wavelength	MASNUM to WRF: significant wave height	WW3 to WRF: Charnock coefficient (Charnock, 1955)
Variables exchanged between the ocean and wave	ROMS to SWAN: surface currents, free surface elevation, and bathymetry	POM to MASNUM: sea surface current	NEMO to WW3: surface current velocity, water level
	SWAN to ROMS: significant wave height, wavelength, wave direction, surface and bottom periods, percent wave breaking, wave energy dissipation, and bottom orbital velocity	MASNUM to POM: Non-breaking wave-induced vertical mixing coefficient	WW3 to NEMO: surface Stokes drift, significant wave height, mean wave period, wave-supported stress, momentum flux from waves to currents, TKE flux from waves to currents

TABLE II. (*Continued.*)

	COAWST (Warner *et al.*, 2010)	FIO-AOW (Zhao *et al.*, 2017)	UU-CM (Wu *et al.*, 2019)
Application examples	Hurricane Ida and Nor'Ida 2009 (Olabarrieta *et al.*, 2012), Hurricane Isabel 2003 (Warner *et al.*, 2010), Hurricane Florence 2018 (Zambon *et al.*, 2021), Typhoon Shanshan 2018 and Megi 2010 (Zhang *et al.*, 2022; Zhang *et al.*, 2023b), Tropical storms in Bay of Bengal (Kiran and Balaji, 2022)	Typhoon Haiyan and Jebi (Zhao *et al.*, 2017), TC Yagi, Leepi, Bebinca, Rumbia, Soulik, Jebi, Utor, Trami, Kong-Rey, Joraji, Usagi, Pabuk, Wutip, Sepat, Fitow, Danas, Nari, Wipha, Francisco, Krosa, Haiyan (Zhao *et al.*, 2022)	Baltic Sea and the North Sea (Wu *et al.*, 2019; Wu *et al.*, 2020)

historical observations and reanalysis data (Emanuel *et al.*, 2008; Hallowell *et al.*, 2018). However, studies incorporating both observations and model simulations have shown that climate change can alter the characteristics of these extreme phenomena, such as the frequency and intensity of hurricanes, as summarized in Sec. V. This implies that the parameters derived from extreme value theory might differ when future climate data are considered and may in fact be non-stationary throughout the lifecycle of an offshore wind farm. Of greater concern is the insurance industry's practice of using onshore locations as proxies in their statistical loss models for offshore claims (Wang *et al.*, 2024). Therefore, the return levels for certain locations should be re-estimated, incorporating additional information from future climate projections provided by climate models. On the other hand, efforts are needed to develop and maintain quality climate datasets with uncertainty estimates. Although confidence on future TC activity on global, and to a lesser extent, basin scales is higher, regional activity is less well understood. In particular, characteristics of future TCs and ETCs over U.S. offshore wind lease areas are not as well understood. Improved representation of physical processes in climate models and better observations are needed as discussed earlier (Secs. VII A and VII B) for enhancing future projections and reducing uncertainties associated with both local and large-scale circulations, as well as SST warming patterns.

In addition, other hurricane-induced hazards could damage the OWTs, although they are not as severe as strong winds and high waves (as described in Sec. VI C). These hazards are not fully understood in the current capacity of modeling and observational studies. These include rainfall drop size distributions, lightning, and other small-scale phenomena such as tornadoes. Studies on rainfall drop size distributions are very limited in time and space. Existing datasets might not cover a wide range of turbine locations and environmental conditions, leading to uncertainties in the assessment of rainfall impacts. The precise mechanisms that trigger lightning within hurricanes are not yet fully understood (Asfur *et al.*, 2020). Accurate representation of updrafts and downdrafts is essential for simulating the vertical transport of charge and the development of lightning. Resolving these processes at the appropriate spatial and temporal scales remains a challenge. The prediction of tornadoes (including waterspouts) is a classic example of scale interaction. It involves large-scale, storm-scale and tornado-scale environments. Modeling these scale interactions is challenging due to limitations in model resolution, understanding of treatment of moist convection, and boundary layer processes among others. Statistical or AI/ML models applied to mesoscale models may offer some hope in improving tornado prediction without needing to do LES to explicitly simulate tornadoes.

ACKNOWLEDGMENTS

This study is supported by the Wind Energy Technologies Office (WETO) of the U.S. Department of Energy (DOE) Office of Energy Efficiency and Renewable Energy. We thank Dr. Steven Brus and Kyle Peco from Argonne for reviewing and formatting the manuscript. Argonne National Laboratory is a U.S. Department of Energy laboratory managed by UChicago Argonne, LLC, under Contract DE-AC02-06CH11357. This work was authored in part by the National Renewable Energy Laboratory, operated by Alliance for Sustainable Energy, LLC, for the U.S. Department of Energy (DOE) under Contract No. DE-AC36-08GO28308. Funding provided by the U.S. Department of Energy Office of Energy Efficiency and Renewable Energy Wind Energy Technologies Office. The views expressed in the article do not necessarily represent the views of the DOE or the U.S. Government. The U.S. Government retains and the publisher, by accepting the article for publication, acknowledges that the U.S. Government retains a nonexclusive, paid-up, irrevocable, worldwide license to publish or reproduce the published form of this work, or allow others to do so, for U.S. Government purposes. The Pacific Northwest National Laboratory is operated for DOE by Battelle Memorial Institute under Contract DE-AC05-76RL01830. This is contribution No. 124 of the Great Lakes Research Center at Michigan Tech. The U.S. National Science Foundation (NSF) National Center for Atmospheric Research (NCAR) is a subcontractor to PNNL under Contract No. 721249. NSF NCAR is a major facility sponsored by the National Science Foundation under Cooperative Agreement No. 1852977.

AUTHOR DECLARATIONS

Conflict of Interest

The authors have no conflicts to disclose.

Author Contributions

Jiali Wang: Conceptualization (equal); Writing – original draft (equal); Writing – review & editing (equal). **Eric Hendricks:** Writing –

original draft (equal); Writing – review & editing (equal). **Christopher M. Rozoff:** Writing – original draft (equal); Writing – review & editing (equal). **Matt Churchfield:** Writing – original draft (equal). **Longhuan Zhu:** Writing – original draft (equal). **Sha Feng:** Writing – original draft (equal). **William J. Pringle:** Writing – original draft (equal). **Mrinal Biswas:** Writing – original draft (supporting). **Sue Ellen Haupt:** Writing – review & editing (equal). **Georgios Deskos:** Writing – review & editing (equal). **Chunyong Jung:** Writing – review & editing (equal). **Pengfei Xue:** Writing – review & editing (supporting). **Larry K. Berg:** Writing – review & editing (supporting). **George Bryan:** Writing – review & editing (supporting). **Branko Kosovic:** Writing – review & editing (supporting). **Rao Kotamarthi:** Writing – review & editing (supporting).

DATA AVAILABILITY

Data sharing is not applicable to this article as no new data were created or analyzed in this study.

APPENDIX: FORMULAS FOR WAVE-INDUCED ROUGHNESS CALCULATION AND THREE FULLY COUPLED ATMOSPHERE-OCEAN-WAVE MODELS

Table I shows formulas for wave-induced roughness (Z_0), where u^* is the friction velocity, H_s is the significant wave height, L_p is wavelength at the peak of the wave spectrum, c_p is the wave phase speed at the peak of the spectrum, and θ is difference of the wind direction and the peak wave direction (in radians). Table II shows three well-validated, fully coupled ocean-atmosphere–wave models: COAWST, FIO-AOW, and UU-CM.

REFERENCES

Aijaz, S., Ghantous, M., Babanin, A. V., Ginis, I., Thomas, B., and Wake, G., "Nonbreaking wave-induced mixing in upper ocean during tropical cyclones using coupled hurricane-ocean-wave modeling," J. Geophysi. Res. **122**(5), 3939–3963 (2017).

Alemany, S., Beltran, J., Perez, A., and Ganzfried, S., "Predicting hurricane trajectories using a recurrent neural network," AAAI Conf. Artif. Intell. **33**, 468–475 (2019).

Alessandrini, S., Delle Monache, L., Rozoff, C. M., and Lewis, W. E., "Probabilistic prediction of tropical cyclone intensity with an analog ensemble," Mon. Weather Rev. **146**, 1723–1744 (2018).

Altman, J., Saurer, M., Dolezal, J., Maredova, N., Song, J.-S., Ho, C.-H., and Treydte, K., "Large volcanic eruptions reduce landfalling tropical cyclone activity: Evidence from tree rings," Sci. Total Environ **775**, 145899 (2021).

Andreas, E. L., "An algorithm to predict the turbulent air-sea fluxes in high-wind, spray conditions," in 12th Conference on Interaction of Sea and Atmosphere (2003).

Andreas, E. L., Mahrt, L., and Vickers, D., "A new drag relation for aerodynamically rough flow over the ocean," J. Atmos. Sci. **69**(8), 2520–2537 (2012).

Andreas, E. L., Mahrt, L., and Vickers, D., "An improved bulk air-sea surface flux algorithm, including spray-mediated transfer," Q. J. R. Meteorol. Soc. **141**(687), 642–654 (2015).

Asfur, M., Price, C., Silverman, J., and Wishkerman, J., "Why is lightning more intense over the oceans?" J. Atmos. Sol.-Terr. Phys. **202**, 105259 (2020).

Baatsen, M., Haarsma, R. J., Van Delden, A. J., and De Vries, H., "Severe autumn storms in future western Europe with a warmer Atlantic Ocean," Clim. Dyn. **45**, 949–964 (2015).

Babanin, A., *Breaking and Dissipation of Ocean Surface Waves* (Cambridge University Press, 2011).

Babanin, A. V., "On a wave-induced turbulence and a wave-mixed upper ocean layer," Geophys. Res. Lett. **33**(20), 1–6, https://doi.org/10.1029/2006GL027308 (2006).

Babanin, A. V. and Haus, B. K., "On the existence of water turbulence induced by nonbreaking surface waves," J. Phys. Oceanogr. **39**(10), 2675–2679 (2009).

Bacmeister, J. T., Wehner, M. F., Neale, R. B., Gettelman, A., Hannay, C., Lauritzen, P. H., Caron, J. M., and Truesdale, J. E., "Exploratory high-resolution climate simulations using the community atmosphere model (CAM)," J. Clim. **27**(9), 3073–3099 (2014).

Baek, Y.-H., Moon, I.-J., Im, J., and Lee, J., "A novel tropical cyclone size estimation model based on a convolutional neural network using geostationary satellite imagery," Remote Sens. **14**, 426–444 (2022).

Balaguru, K., Xu, W., Chang, C. C., Leung, L. R., Judi, D. R., Hagos, S. M., Wehner, M. F., Kossin, J. P., and Ting, M., "Increased U.S. coastal hurricane risk under climate change," Sci. Adv. **9**(14), eadf0259 (2023).

Balaguru, K., Leung, L. R., Van Roekel, L. P., Golaz, J. C., Ullrich, P. A., Caldwell, P. M., Hagos, S. M., Harrop, B. E., and Mametjanov, A., "Characterizing tropical cyclones in the energy exascale earth system model version 1," J. Adv. Model. Earth Syst. **12**(8), e2019MS002024 (2020).

Bao, Y., Song, Z., and Qiao, F., "FIO-ESM version 2.0: Model description and evaluation," J. Geophys. Res. **125**(6), e2019JC016036, https://doi.org/10.1029/2019JC016036 (2020).

Barthelmie, R. J., Dantuono, K. E., Renner, E. J., Letson, F. L., and Pryor, S. C., "Extreme wind and waves in U.S. east coast offshore wind energy lease areas," Energies **14**(4), 1053 (2021).

Bender, M. A. and Ginis, I., "Real-case simulations of hurricane–ocean interaction using a high-resolution coupled model: Effects on hurricane intensity," Mon. Weather Rev. **128**(4), 917–946 (2000).

Bernardet, L., Tallapragada, V., Bao, S., Trahan, S., Kwon, Y., Liu, Q., Tong, M., Biswas, M., Brown, T., Stark, D., and Carson, L., "Community support and transition of research to operations for the hurricane weather research and forecasting model," Bull. Am. Meteorol. Soc. **96**(6), 953–960 (2015).

Best, A. C., "The size distribution of raindrops," Meteorol. Soc **76**, 16–36 (1950).

Bethel, B. J., Sun, W., Dong, C., and Wang, D., "Forecasting hurricane-forced significant wave heights using a long short-term memory network in the Caribbean Sea," Ocean Sci. **18**, 419–436 (2022).

Bhatia, K. T., Vecchi, G. A., Knutson, T. R., Murakami, H., Kossin, J., Dixon, K. W., and Whitlock, C. E., "Recent increases in tropical cyclone intensification rates," Nat. Commun. **10**(1), 635 (2019).

Bi, K., Xie, L., Zhang, H. *et al.*, "Accurate medium-range global weather forecasting with 3D neural networks," Nature **619**, 533–538 (2023).

Bloemendaal, N., De Moel, H., Muis, S., Haigh, I. D., and Aerts, J. C., "Estimation of global tropical cyclone wind speed probabilities using the STORM dataset," Sci. Data **7**(1), 1–11 (2020).

Bloemendaal, N., De Moel, H., Martinez, A. B., Muis, S., Haigh, I. D., van der Wiel, K., Haarsma, R. J., Ward, P. J., Roberts, M. J., Dullaart, J. C., and Aerts, J. C., "A globally consistent local-scale assessment of future tropical cyclone risk," Sci. Adv. **8**(17), eabm8438 (2022).

Blumberg, A. F. and Mellor, G. L., "A description of a three-dimensional coastal ocean circulation model," in *Three-Dimensional Coastal Ocean Models*, Coastal and Estuarine Sciences series (Wiley, 1987), Vol. 4, pp. 1–16.

Booij, N., Ris, R. C., and Holthuijsen, L. H., "A third-generation wave model for coastal regions 1. Model description and validation," J. Geophys. Res. **104**(C4), 7649–7666, https://doi.org/10.1029/98JC02622 (1999).

Bose, R., Pintar, A., and Simju, E., "A real time prediction methodology for hurricane evolution using LSTM recurrent neural networks," Neural Comput. Appl. **34**, 17491–17505 (2022).

Breivik, Ø., Mogensen, K., Bidlot, J., Balmaseda, M. A., and Janssen, P. A. E. M., "Surface wave effects in the NEMO ocean model: Forced and coupled experiments," J. Geophys. Res. **120**(4), 2973–2992, https://doi.org/10.1002/2014JC010565 (2015).

Bruneau, N., Toumi, R., and Wang, S., "Impact of wave whitecapping on land falling tropical cyclones," Sci. Rep. **8**(1), 1–11 (2018).

Brus, S. R., Wolfram, P. J., Van Roekel, L. P., and Meixner, J. D., "Unstructured global to coastal wave modeling for the Energy Exascale Earth System Model using WAVEWATCH III version 6.07," Geosci. Model Dev. **14**, 2917–2938 (2021).

Bryan, G. H., Worsnop, R. P., Lundquist, J. K., and Zhang, J. A., "A simple method for simulating wind profiles in the boundary layer of tropical cyclones," Boundary-Layer Meteorol. **162**, 475–502 (2017).
Bucci, L. R., O'Handley, C., Emmitt, G. D., Zhang, J. A., Ryan, K., and Atlas, R., "Validation of an airborne Doppler wind Lidar in tropical cyclones," Sensors **18**(12), 4288 (2018).
Buchana, P. and McSharry, P. E., "Windstorm risk assessment for offshore wind farms in the North Sea," Wind Energy **22**, 1219–1229 (2019).
Burchard, H., "Simulating the wave-enhanced layer under breaking surface waves with two-equation turbulence models," J. Phys. Oceanogr. **31**(11), 3133–3145 (2001).
Caldwell, P. M., Mametjanov, A., Tang, Q., Van Roekel, L. P., Golaz, J. C., Lin, W. *et al.*, "The DOE E3SM coupled model version 1: Description and results at high resolution," J. Adv. Model. Earth Syst. **11**(12), 4095–4146 (2019).
Camargo, S. J., "Global and regional aspects of tropical cyclone activity in the CMIP5 models," J. Clim. **26**(24), 9880–9902 (2013).
Camargo, S. J., Giulivi, C. F., Sobel, A. H., Wing, A. A., Kim, D., Moon, Y. *et al.*, "Characteristics of model tropical cyclone climatology and the large-scale environment," J. Clim. **33**(11), 4463–4487 (2020).
Cangialosi, J. P., see https://www.nhc.noaa.gov/verification/pdfs/Verification_2022.pdf for "National hurricane center forecast verification report for 2022 hurricane season" (2023).
Cavaleri, L., Fox-Kemper, B., and Hemer, M., "Wind waves in the coupled climate system," Bull. Am. Meteorol. Soc. **93**(11), 1651–1661 (2012).
Chand, S. S., Walsh, K. J. E., Camargo, S. J., Kossin, J. P., Tory, K. J., Wehner, M. F. *et al.*, "Declining tropical cyclone frequency under global warming," Nat. Clim. Change **12**(7), 655–661 (2022).
Charnock, H., "Wind stress on a water surface," Q. J. R. Meteorol. Soc. **81**(350), 639–640 (1955).
Chauvin, F., Pilon, R., Palany, P., and Belmadani, A., "Future changes in Atlantic hurricanes with the rotated-stretched ARPEGE-Climat at very high resolution," Clim. Dyn. **54**, 947–972 (2020).
Chavas, D. R., Lin, N., and Emanuel, K., "A model for the complete radial structure of the tropical cyclone wind field. Part I: Comparison with observed structure," J. Atmos. Sci. **72**, 3647–3662 (2015).
Chen, L., Zhong, X., Zhang, F., Cheng, Y., Xu, Y., Qi, Y., and Li, H., "FuXi: A cascade machine learning forecasting system for 15-day global weather forecast," npj Clim. Atmos. Sci. **6**(1), 190 (2023).
Chen, B.-F., Chen, B., Lin, H. T., and Elsberry, R. L., "Estimating tropical cyclone intensity by satellite imagery utilizing convolutional neural networks," Weather Forecast. **34**, 447–465 (2019).
Chen, B.-F., Kuo, Y.-T., and Huang, T.-S., "A deep learning ensemble approach for predicting tropical cyclone rapid intensification," Atmos. Sci. Lett. **24**, e1151 (2023).
Chen, S. S., Price, J. F., Zhao, W., Donelan, M. A., and Walsh, E. J., "The CBLAST-hurricane program and the next-generation fully coupled atmosphere–wave–ocean models for hurricane research and prediction," Bull. Am. Meteorol. Soc. **88**(3), 311–318 (2007).
Chen, S. S., Zhao, W., Donelan, M. A., and Tolman, H. L., "Directional wind–wave coupling in fully coupled atmosphere–wave–ocean models: Results from CBLAST-Hurricane," J. Atmos. Sci. **70**(10), 3198–3215 (2013).
Chen, Y. and Yu, X., "Enhancement of wind stress evaluation method under storm conditions," Climate Dynam. **47**, 3833–3843 (2016).
Chen, S. S. and Curcic, M., "Coupled modeling and observations of ocean surface waves in Hurricane Ike (2008) and Superstorm Sandy (2012)," Ocean Modeling (2016). **103**, 161–173.
Chen, S.-T., "Probabilistic forecasting of coastal wave height during typhoon warning period using machine learning methods," Hydroinformatics **21**, 343–358 (2019).
Chen, X. and Xu, J.-Z., "Structural failure analysis of wind turbines impacted by super typhoon Usagi," Eng. Failure Anal. **60**, 391–404 (2016).
Chen, Y. and Yu, X., "Sensitivity of storm wave modeling to wind stress evaluation methods," J. Adv. Model. Earth Syst. **9**(2), 893–907 (2017).
Chen, X., Bryan, G. H., Zhang, J. A., Cione, J. J., and Marks, F. D., "A framework for simulating the tropical cyclone boundary layer using large-eddy simulation and its use in evaluating PBL parameterizations," J. Atmos. Sci. **78**, 3559–3574 (2021).
Cheung, H. M., Ho, C.-H., and Chang, M., "Hybrid neural network models for postprocessing medium-range forecasts of tropical cyclone tracks over the Western North Pacific," Artif. Intell. Earth Syst. **1**, e210003 (2022).
Cloud, K. A., Reich, B. J., Rozoff, C. M., Alessandrini, S., Lewis, W. E., and Delle Monache, L., "A feed forward neural network based on model output statistics for short-term hurricane intensity prediction," Weather Forecast. **34**, 985–997 (2019).
Colle, B. A., Zhang, Z., Lombardo, K. A., Chang, E., Liu, P., and Zhang, M., "Historical evaluation and future prediction of eastern North American and Western Atlantic extratropical cyclones in the CMIP5 models during the cool season," J. Clim. **26**(18), 6882–6903 (2013).
Craig, A., Valcke, S., and Coquart, L., "Development and performance of a new version of the OASIS coupler. OASIS3-MCT-3.0," Geosci. Model Dev. **10**(9), 3297–3308 (2017).
Craig, P. D. and Banner, M. L., "Modeling wave-enhanced turbulence in the ocean surface layer," J. Phys. Oceanogr. **24**(12), 2546–2559 (1994).
D'Alessio, S. J. D., Abdella, K., and McFarlane, N. A., "A new second-order turbulence closure scheme for modeling the oceanic mixed layer," J. Phys. Oceanogr. **28**(8), 1624–1641 (1998).
Davis, C., Wang, W., Chen, S. S., Chen, Y., Corbosiero, K., DeMaria, M., Dudhia, J., Holland, G., Klemp, J., Michalakes, J., Reeves, H., Rotunno, R., Synder, C., and Xiao, Q., "Prediction of landfalling hurricanes with the advanced hurricane WRF model," Mon. Weather Rev. **136**(6), 1990–2005 (2008).
Dettling, S. M., Brummet, T., Gagne, D. J., Kosovic, B., Haupt, S. E., and Hawbecker, P., "Downscaling from mesoscale to microscale in complex terrain using a generative adversarial network," in *102nd American Meteorological Society Annual Meeting*, Jan 25 (AMS, 2022).
Diamond, K. E., "Extreme weather impacts on offshore wind turbines: Lessons learned," Nat. Resour. Environ. **27**, 37 (2012).
Domala, V., Lee, W., and Kim, T.-W., "Wave data prediction with optimized machine learning and deep learning techniques," J. Comput. Des. Eng. **9**, 1107–1122 (2022).
Donelan, M. A., "On the limiting aerodynamic roughness of the ocean in very strong winds," Geophys. Res. Lett. **31**(18), L18306, https://doi.org/10.1029/2004GL019460 (2004).
Dong, C., Loy, C. C., He, K., and Tang, X., "Learning a deep convolutional network for image super-resolution," in *European Conference on Computer Vision* (Springer, 2014), pp. 184–199.
Dong, L. and Zhang, F., "OBEST: An observation-based ensemble subsetting technique for tropical cyclone track prediction," Weather Forecast. **31**, 57–70 (2016).
Drennan, W. M., Graber, H. C., Hauser, D., and Quentin, C., "On the wave age dependence of wind stress over pure wind seas," J. Geophys. Res. **108**(C3), 8062, https://doi.org/10.1029/2000JC000715 (2003).
Drennan, W. M., Taylor, P. K., and Yelland, M. J., "Parameterizing the sea surface roughness," J. Phys. Oceanogr. **35**(5), 835–848 (2005).
Du, J., Bolaños, R., and Guo Larsén, X., "The use of a wave boundary layer model in SWAN," J. Geophys. Res. **122**(1), 42–62, https://doi.org/10.1002/2016JC012104 (2017).
Du, J., Larsén, X. G., Chen, S., Bolaños, R., Badger, M., and Yang, Y., "The impact of wind–wave coupling with WBLM on coastal storm simulations," Ocean Modell. **180**, 102135 (2022).
Dyer, A. S., Zaengle, D., Nelson, J. R., Duran, R., Wenzlick, M., Wingo, P. C., Bauer, J. R., Rose, K., and Romeo, L., "Applied machine learning model comparison: Predicting offshore platform integrity with gradient boosting algorithms and neural networks," Mar. Struct. **83**, 103152 (2021).
Edwards, R. and Mosier, R. M., "Over a quarter century of TCTOR: Tropical cyclone tornadoes in the WSR-88D ERA," in *30th Conference on Severe Local Storms*, Santa Fe, NM (American Meteorological Society, 2022), P171.
Elsner, J. B., "Continued increases in the intensity of strong tropical cyclones," Bull. Am. Meteorol. Soc. **101**, E1301–E1303 (2020).
Emanuel, K., "Response of global tropical cyclone activity to increasing CO_2: Results from downscaling CMIP6 models," J. Clim. **34**(1), 57–70 (2021).
Emanuel, K., Sundararajan, R., and Williams, J., "Hurricanes and global warming: Results from downscaling IPCC AR4 simulations," Bull. Amer. Meteor. Soc. **89**, 347–368 (2008).

Emanuel, K., "Climate and tropical cyclone activity: A new model downscaling approach," J. Clim. **19**(19), 4797–4802 (2006).
Emanuel, K. A., Ravela, S., Vivant, E., and Risi, C., "A statistical-deterministic approach to hurricane risk assessment," Bull. Am. Meteor. Soc. **87**, 299–314 (2006).
Emanuel, K., "Evidence that hurricanes are getting stronger," Proc. Natl. Acad. Sci. **117**, 13194–13195 (2020).
Evans, C. *et al.*, "The extratropical transition of tropical cyclones. Part I: Cyclone evolution and direct impacts," Mon. Weather Rev. **145**, 4317–4344 (2017).
Fairall, C. W., Kepert, J. D., and Holland, G. J., "The effect of sea spray on surface energy transports over the ocean," Global Atmos. Ocean Syst. **2**, 121–142 (1994).
Fan, Y. and Griffies, S. M., "Impacts of parameterized Langmuir turbulence and nonbreaking wave mixing in global climate simulations," J. Clim. **27**(12), 4752–4775 (2014).
Foster, R. C., "Why rolls are prevalent in the hurricane boundary layer," J. Atmos. Sci. **62**, 2647–2661 (2005).
Fowle, M. A. and Roebber, P. J., "Short-range (0–48 h) numerical prediction of convective occurrence, mode, and location," Weather Forecast. **18**(5), 782–794 (2003).
Gall, R., Tuttle, J., and Hildebrand, P., "Small-scale spiral bands observed in hurricanes Andrew, Hugo, and Erin," Mon. Weather Rev. **126**(7), 1749–1766 (1998).
Gao, S., Zhao, P., Pan, B., Li, Y., Zhou, M., Xu, J., Zhong, S., and Shi, Z., "A nowcasting model for the prediction of typhoon tracks based on a long short term memory neural network," Acta. Oceanog. Sin. **37**, 8–12 (2018).
Gao, D., Pan, X., Liang, B., Yang, B., Wu, G., and Wang, Z., "A review and design principle of fixed-bottom foundation scour protection schemes for offshore wind energy," J. Mar. Sci. Eng. **12**(4), 660 (2024).
Garolera, A. C., Madsen, S. F., Nissim, M., Myers, J. D., and Hollboell, J., "Lightning damage to wind turbine blades from wind farms in the U.S," IEEE Trans. Power Delivery **31**(3), 1043–1049 (2016).
Ghantous, M. and Babanin, A. V., "One-dimensional modelling of upper ocean mixing by turbulence due to wave orbital motion," Nonlinear Processes Geophys. **21**(1), 325–338 (2014).
Giffard-Roisin, S., Yang, M., Charpiat, G., Kumler Bonfanti, C., Kegl, B., and Monteleoni, C., "Tropical cyclone track forecasting using fused deep learning from aligned reanalysis data," Front. Big Data **3**, 1 (2020).
Golaz, J. C., Caldwell, P. M., Van Roekel, L. P., Petersen, M. R., Tang, Q., Wolfe, J. D. *et al.*, "The DOE E3SM coupled model version 1: Overview and evaluation at standard resolution," J. Adv. Model. Earth Syst. **11**(7), 2089–2129 (2019).
Goodfellow, I., Pouget-Abadie, J., Mirza, M., Xu, B., Warde-Farley, D., Ozair, S., Courville, A., and Bengio, Y., "Generative adversarial nets," in Advances in Neural Information Processing Systems 27 (NIPS 2014) (2014).
Gopalakrishnan, S. G., Goldenberg, S., Quirino, T., Zhang, X., Marks, F., Yeh, K. S., Atlas, R., and Tallapragada, V., "Toward improving high-resolution numerical hurricane forecasting: Influence of model horizontal grid resolution, initialization, and physics," Weather Forecast. **27**(3), 647–666 (2012).
Gray, W. M., "Atlantic seasonal hurricane frequency. Part I: El Niño and 30 mb quasi-biennial oscillation influences," Mon. Weather Rev. **112**, 1649–1668 (1984).
Griffin, S. M., Wimmers, A., and Velden, C. S., "Predicting rapid intensification in North Atlantic and Eastern North Pacific tropical cyclones using a convolutional neural network," Weather Forecast. **37**, 1333–1355 (2022).
Gurung, I., Ramsubhramanian, M., Freitag, B., Kaulfus, A., Maskey, M., Ramachandran, R., and Alemohammad, H., "Tropical cyclone wind speed estimation: A large scale training data set and community benchmarking," Earth Space Sci. **10**, e2022EA002693 (2023).
Haarsma, R. J., Hazeleger, W., Severijns, C., De Vries, H., Sterl, A., Bintanja, R., Van Oldenborgh, G. J., and Van Den Brink, H. W., "More hurricanes to hit western Europe due to global warming," Geophys. Res. Lett. **40**(9), 1783–1788, https://doi.org/10.1002/grl.50360 (2013).
Haarsma, R. J., Roberts, M. J., Vidale, P. L., Catherine, A., Bellucci, A., Bao, Q. *et al.*, "High resolution model intercomparison project (HighResMIP v1.0) for CMIP6," Geosci. Model Dev. **9**(11), 4185–4208 (2016).
Haidvogel, D. B., Arango, H., Budgell, W. P., Cornuelle, B. D., Curchitser, E., Di Lorenzo, E., Fennel, K., Geyer, W. R., Hermann, A. J., Lanerolle, L., Levin, J., McWilliams, J. C., Miller, A. J., Moore, A. M., Powell, T. M., Shchepetkin, A. F., Sherwood, C. R., Signell, R. P., Warner, J. C., and Wilkin, J., "Ocean forecasting in terrain-following coordinates: Formulation and skill assessment of the Regional Ocean Modeling System," J. Comput. Phys. **227**(7), 3595–3624 (2008).
Hallowell, S. T., Myers, A. T., Arwade, S. R., Pang, W., Rawal, P., Hines, E. M. *et al.*, "Hurricane risk assessment of offshore wind turbines," Renewable Energy **125**, 234–249 (2018).
Haupt, S. E., Chapman, W., Adams, S. V., Kirkwood, C., Hosking, J. S., Robinson, N. H., Lerch, S., and Subramanian, A. C., "Towards implementing artificial intelligence post-processing in weather and climate: Proposed actions from the Oxford 2019 workshop," Philos. Trans. R. Soc. A **379**(2194), 20200091 (2021).
He, J. Y., Chan, P. W., Li, Q. S., Li, L., Zhang, L., and Yang, H. L., "Observations of wind and turbulence structures of Super Typhoons Hato and Mangkhut over land from a 356 m high meteorological tower," Atmos. Res. **265**, 105910 (2022).
Herndon, D. and Langlade, S., see https://community.wmo.int/en/iwtc-10-reports for "Topic 1: Remote sensing for tropical cyclone analysis" (2022).
Herring, R., Dyer, K., Howkins, P., and Ward, C., "Characterisation of the offshore precipitation environment to help combat leading edge erosion of wind turbine blades," Wind Energy Sci. **5**, 1399–1409 (2020).
Hersbach, H., Bell, B., Berrisford, P., Hirahara, S., Horányi, A., Muñoz-Sabater, J., Nicolas, J., Peubey, C., Radu, R., Schepers, D., and Simmons, A., "The ERA5 global reanalysis," Q. J. R. Meteorol. Soc. **146**(730), 1999–2049 (2020).
Hoarau, T., Barthe, C., Tulet, P., Claeys, M., Pinty, J. P., Bousquet, O. *et al.*, "Impact of the generation and activation of sea salt aerosols on the evolution of tropical cyclone Dumile," J. Geophys. Res. **123**(16), 8813–8831, https://doi.org/10.1029/2017JD028125 (2018).
Holbach, H. M., Bousquet, O., Bucci, L., Chang, P., Cione, J., Ditchek, S., Doyle, J., Duvel, J. P., Elston, J., Goni, G., and Hon, K. K., "Recent advancements in aircraft and in situ observations of tropical cyclones," Trop. Cyclone Res. Rev. **12**(2), 81–99 (2023).
Holbach, H. and Bousquet, O., see https://community.wmo.int/en/iwtc-10-reports for "Topic 1.3: Advancements in aircraft and in-situ observations of tropical cyclones" (2022).
Holzworth, R. H., McCarthy, M. P., Brundell, J. B., Jacobson, A. R., and Rodger, C. J., "Global distribution of superbolts," J. Geophys. Res. **124**(17–18), 9996–10005, https://doi.org/10.1029/2019JD030975 (2019).
Hsu, T.-Y., Shiao, S.-Y., and Liao, W.-I., "Damage detection of rotating wind turbine blades using local flexibility method and long-gauge fiber Bragg grating sensors," Meas. Sci. Technol. **29**(1), 2018 (2018).
Huang, C. J., Qiao, F., Song, Z., and Ezer, T., "Improving simulations of the upper ocean by inclusion of surface waves in the Mellor-Yamada turbulence scheme," J. Geophys. Res. **116**(C1), C01007, https://doi.org/10.1029/2010JC006320 (2011).
Huang, L., Li, X., Liu, B., Zhang, J. A., Shen, D., Zhang, Z., and Yu, W., "Tropical cyclone boundary layer rolls in synthetic aperture radar imagery," J. Geophys. Res. **123**(4), 2981–2996, https://doi.org/10.1029/2018JC013755 (2018).
Huang, Y. and Jin, L., "A prediction scheme with genetic neural network and Isomap algorithm for tropical cyclone intensity change over western North Pacific," Meteorol. Atmos. Phys. **121**, 143–152 (2013).
IEC, "Wind turbines—Part 3: Design requirements for offshore wind turbines," No. IEC 61400-3-1:2019, 2019.
Ikuyajolu, O. J., Van Roekel, L., Brus, S. R., Thomas, E. E., Deng, Y., and Benedict, J. J., "Effects of surface turbulence flux parameterizations on the MJO: The role of ocean surface waves," J. Clim. **37**(10), 3011–3036 (2024).
Ikuyajolu, O. J., Van Roekel, L., Brus, S. R., Thomas, E. E., Deng, Y., and Sreepathi, S., "Porting the WAVEWATCH III (v6.07) wave action source terms to GPU," Geosci. Model Dev. **16**(4), 1445–1458 (2023).
Ito, J., Oizume, T., and Niino, H., "Near-surface coherent structures explored by large eddy simulation of entire tropical cyclones," Sci. Rep. **7**, 3798 (2017).
Jacob, R., Larson, J., and Ong, E., "M × N communication and parallel interpolation in community climate system model version 3 using the model coupling toolkit," Int. J. High Perform. Comput. Appl. **19**(3), 293–307 (2005).

Janssen, P. A. E. M., "Wave-induced stress and the drag of air flow over sea waves," J. Phys. Oceanogr. **19**(6), 745–754 (1989).
Janssen, P. A. E. M., "Quasi-linear theory of wind-wave generation applied to wave forecasting," J. Phys. Oceanogr. **21**(11), 1631–1642 (1991).
Jiang, S., Fan, H., and Wang, C., "Improvement of typhoon intensity forecasting by using a novel spatio-temporal deep learning model," Remote Sens. **14**, 5205 (2022).
Jones, S. C., Harr, P. A., Abraham, J., Bosart, L. F., Bowyer, P. J., Evans, J. L. *et al.*, "The extratropical transition of tropical cyclones: Forecast challenges, current understanding, and future directions," Weather Forecast. **18**(6), 1052–1092 (2003).
Julian, P. R. and Chervin, R. M., "A study of the southern oscillation and Walker circulation phenomenon," Mon. Weather Rev. **106**, 1433–1451 (1978).
Jung, C. and Lackmann, G. M., "Extratropical transition of Hurricane Irene (2011) in a changing climate," J. Clim. **32**, 4847–4871 (2019).
Jung, C. and Lackmann, G. M., "The response of extratropical transition of tropical cyclones to climate change: Quasi-idealized numerical experiments," J. Clim. **34**, 4361–4381 (2021).
Jung, C. and Lackmann, G. M., "Changes in tropical cyclones undergoing extratropical transition in a warming climate: Quasi-idealized numerical experiments of North Atlantic landfalling events," Geophys. Res. Lett. **50**, e2022GL101963, https://doi.org/10.1029/2022GL101963 (2023).
Kantha, L. H. and Clayson, C. A., "An improved mixed layer model for geophysical applications," J. Geophys. Res. **99**(C12), 25235, https://doi.org/10.1029/94JC02257 (1994).
Kapoor, A., Ouakka, S., Arwade, S. R., Lundquist, J. K., Lackner, M. A., Myers, A. T., Worsnop, R. P., and Bryan, G. H., "Hurricane eyewall winds and structural response of wind turbines," Wind Energy Sci. **5**, 89–104 (2020).
Kim, E. and Manuel, L., "Hurricane risk assessment for offshore wind plants," Wind Eng. **40**(3), 261–269 (2016).
Kim, H. S., Vecchi, G. A., Knutson, T. R., Anderson, W. G., Delworth, T. L., Rosati, A., Zeng, F., and Zhao, M., "Tropical cyclone simulation and response to CO_2 doubling in the GFDL CM2.5 high-resolution coupled climate model," J. Clim. **27**(21), 8034–8054 (2014).
Kiran, P. V. and Balaji, C., "The future projection of cyclones in Bay of Bengal: A study using coupled ocean atmosphere model," Ocean Dyn. **72**, 641–660 (2022).
Klotzbach, P. J., Wood, K. M., Schreck, C. J. III, Bowen, S. G., Patricola, C. M., and Bell, M. M., "Trends in global tropical cyclone activity: 1990–2021," Geophys. Res. Lett **49**, e2021GL095774, https://doi.org/10.1029/2021GL095774 (2022).
Knutson, T., Camargo, S. J., Chan, J. C., Emanuel, K., Ho, C. H., Kossin, J. *et al.*, "Tropical cyclones and climate change assessment," Bull. Am. Meteorol. Soc. **101**(3), E303–E322 (2020).
Knutson, T. R., Sirutis, J. J., Garner, S. T., Held, I. M., and Tuleya, R. E., "Simulation of the recent multidecadal increase of Atlantic hurricane activity using an 18-km-grid regional model," Bull. Am. Meteorol. Soc. **88**(10), 1549–1565 (2007).
Kordmahalleh, M. M., Sefidmazgi, M. G., and Homaifar, A., "A sparse recurrent neural network for trajectory prediction of Atlantic hurricanes," in Proceedings of the Genetic and Evolutionary Computation Conference (2016).
Kossin, J. P., "A global slowdown of tropical-cyclone translation speed," Nature **558**(7708), 104–107 (2018).
Kossin, J. P., Knapp, K. R., Olander, T. L., and Velden, C. S., "Global increase in major tropical cyclone exceedance probability over the past four decades," Proc. Natl. Acad. Sci. **117**, 11975–11980 (2020).
Krishnamurti, T. N. and Bhalme, H. N., "Oscillations of a monsoon system. Part I. Observational aspects," J. Atmos. Sci. **33**, 1937–1954 (1976).
Kumar, S., Dube, A., Ashrit, R., and Mitra, A. K., "A machine learning (ML)-based approach to improve tropical cyclone intensity prediction of NCMRWF ensemble prediction system," Pure Appl. Geophys. **180**(1), 261–275 (2023).
Kurinchi-Vendhan, R., see https://rupakv.com/pdfs/wirediff_report.pdf for "WiREDiff: A wind resolution-enhancing diffusion model" (2023).
Lam, R., Sanchez-Gonzalez, A., Willson, M., Wirnsberger, P., Fortunato, M., Alet, F., Ravuri, S., Ewalds, T., Eaton-Rosen, Z., Hu, W., and Merose, A., "Learning skillful medium-range global weather forecasting," Science **382**(6677), 1416–1421 (2023).
Lane, E. M., Restrepo, J. M., and McWilliams, J. C., "Wave–current interaction: A comparison of radiation-stress and vortex-force," J. Phys. Oceanogr. **37**, 1122–1141 (2007).
Large, W. G. and Pond, S., "Open ocean momentum flux measurements in moderate to strong winds," J. Phys. Oceanogr. **11**(3), 324–336 (1981).
Larson, J., Jacob, R., and Ong, E., "The model coupling toolkit: A new Fortran90 toolkit for building multiphysics parallel coupled models," Int. J. High Perform. Comput. Appl. **19**(3), 277–292 (2005).
Larsén, X. G., Du, J., Bolaños, R., Imberger, M., Kelly, M. C., Badger, M., and Larsen, S., "Estimation of offshore extreme wind from wind-wave coupled modeling," Wind Energy **22**(8), 1043–1057 (2019).
Law Chune, S. and Aouf, L., "Wave effects in global ocean modeling: Parametrizations vs. forcing from a wave model," Ocean Dyn. **68**(12), 1739–1758 (2018).
Ledig, C., Theis, L., Huszár, F., Caballero, J., Cunningham, A., Acosta, A., Aitken, A., Tejani, A., Totz, J., Wang, Z., and Shi, W., "Photo-realistic single image super-resolution using a generative adversarial network," in *IEEE Conference on Computer Vision and Pattern Recognition*, Honolulu, HI (IEEE, 2017), pp. 4681–4690.
Lee, C. Y., Tippett, M. K., Sobel, A. H., and Camargo, S. J., "An environmentally forced tropical cyclone hazard model," J. Adv. Model. Earth Syst. **10**(1), 223–241 (2018).
Lee, J., Im, J., Cha, D.-H., Park, H., and Sim, S., "Tropical cyclone intensity estimation using multi-dimensional convolutional neural networks from geostationary satellite data," Remote Sens. **12**, 108 (2020).
Letson, F. W., Barthelmie, R. J., Hodges, K. I., and Pryor, S. C., "Intense windstorms in the northeastern United States," Nat. Hazards Earth Syst. Sci. **21**(7), 2001–2020 (2021).
Lewis, W. E., Rozoff, C., Alessandrini, S., and Delle Monache, L., "Performance of the HWRF Rapid Intensification Analog Ensemble (HWRF RI-AnEn) during the 2017 and 2018 HFIP real-time demonstrations," Weather Forecast. **35**, 841–856 (2020).
Li, L. and Chakraborty, P., "Slower decay of landfalling hurricanes in a warming world," Nature **587**, 230–234 (2020).
Li, Q., Webb, A., Fox-Kemper, B., Craig, A., Danabasoglu, G., Large, W. G., and Vertenstein, M., "Langmuir mixing effects on global climate: WAVEWATCH III in CESM," Ocean Modell. **103**, 145–160 (2016).
Li, X., Pu, Z., and Gao, Z., "Effects of roll vortices on the evolution of hurricane Harvey during landfall," J. Atmos. Sci. **78**(6), 1847–1867 (2021).
Li, X. and Pu, Z., "Dynamic mechanisms associated with the structure and evolution of roll vortices and coherent turbulence in the hurricane boundary layer: A large eddy simulation during the landfall of hurricane Harvey," Boundary-Layer Meteorol. **186**, 615–636 (2023).
Li, Y., Peng, S., Wang, J., and Yan, J., "Impacts of nonbreaking wave-stirring-induced mixing on the upper ocean thermal structure and typhoon intensity in the South China Sea," J. Geophys. Res. **119**(8), 5052–5070, https://doi.org/10.1002/2014JC009956 (2014).
Lighthill, J., "Ocean spray and the thermodynamics of tropical cyclones," J. Eng. Math. **35**(1–2), 11–42 (1999).
Lin, J., Emanuel, K., and Vigh, J. L., "Forecasts of hurricanes using large-ensemble outputs," Weather Forecast. **35**, 1713–1731 (2020).
Liu, B., Liu, H., Xie, L., Guan, C., and Zhao, D., "A coupled atmosphere–wave–ocean modeling system: Simulation of the intensity of an idealized tropical cyclone," Mon. Weather Rev. **139**(1), 132–152 (2011).
Liu, F., "Projections of future US design wind speeds due to climate change for estimating hurricane losses," Ph.D. thesis (Clemson University, 2014).
Liu, L., Yang, G., Wang, B., Zhang, C., Li, R., Zhang, Z., Ji, Y., and Wang, L., "C-Coupler1: A Chinese community coupler for Earth system modeling," Geosci. Model Dev. **7**(5), 2281–2302 (2014).
Liu, C., Ikeda, K., Rasmussen, R., Barlage, M., Newman, A. J., Prein, A. F. *et al.*, "Continental-scale convection-permitting modeling of the current and future climate of North America," Clim. Dyn. **49**, 71–95 (2017).
Lopez Ortiz, J. P., "Effects of wind turbine rotor positioning on tornado induced loads," M.S. thesis (The University of Western Ontario, 2023).
Lu, X., Wong, W.-K., Yu, H., and Yang, X., "Tropical cyclone size identification over the Western North Pacific using support vector machine and general regression neural network," J. Meteorol. Soc. Jpn. **100**, 927–941 (2022).

Ma, T. and Sun, C., "Large eddy simulation of hurricane boundary layer turbulence and its application for power transmission system," J. Wind Eng. Ind. Aerodyn. **210**, 104520 (2021).

Madden, R. A. and Julian, P. R., "Description of global-scale circulation cells in the tropics with a 40–50 day period," J. Atmos. Sci. **29**, 1109–1123 (1972).

Madec, G. and NEMO Team, see https://www.nemo-ocean.eu/wp-content/uploads/NEMO_book.pdf for "Nemo Ocean Engine" (2016); accessed Aug 01 2023.

Mafi, S. and Amirinia, G., "Forecasting hurricane wave height in Gulf of Mexico using soft computing methods," Ocean Eng. **146**, 352–362 (2017).

Makin, V. K., "A note on the drag of the sea surface at hurricane winds," Boundary-Layer Meteorol. **115**(1), 169–176 (2005).

Mann, M. E., Woodruff, J. D., Donnelly, J. P., and Zhang, Z., "Atlantic hurricanes and climate over the past 1,500 years," Nature **460**(7257), 880–883 (2009).

Martin, P. J., "Simulation of the mixed layer at OWS November and Papa with several models," J. Geophys. Res. **90**(C1), 903, https://doi.org/10.1029/JC090iC01p00903 (1985).

Marciano, C. G., Lackmann, G. M., and Robinson, W. A., "Changes in US East Coast cyclone dynamics with climate change," J. Clim. **28**(2), 468–484 (2015).

Mehra, A., Tallapragada, V., Zhang, Z., Liu, B., Zhu, L., Wang, W., and Kim, H. S., "Advancing the state of the art in operational tropical cyclone forecasting at NCEP," Trop. Cyclone Res. Rev. **7**(1), 51–56 (2018).

Mellor, G., "On theories dealing with the interaction of surface waves and ocean circulation," J. Geophys. Res. **121**(7), 4474–4486, https://doi.org/10.1002/2016JC011768 (2016).

Mellor, G. and Blumberg, A., "Wave breaking and ocean surface layer thermal response," J. Phys. Oceanogr. **34**(3), 693–698 (2004).

Meng, F., Song, T., Xu, D., Xie, P., and Li, Y., "Forecasting tropical cyclones wave height using bidirectional gated recurrent unit," Ocean Eng. **234**, 108795 (2021).

Moon, I.-J., Ginis, I., and Hara, T., "Effect of surface waves on air–sea momentum exchange. Part II: Behavior of drag coefficient under tropical cyclones," J. Atmos. Sci. **61**(19), 2334–2348 (2004).

Heming, J. T., Prates, F., Bender, M. A., Bowyer, R., Cangialosi, J., Caroff, P. *et al.*, "Review of recent progress in tropical cyclone track forecasting and expression of uncertainties," Trop. Cyclone Res. Rev. **8**(4), 181–218 (2019).

Michaelis, A. C. and Lackmann, G. M., "Storm-scale dynamical changes of extratropical transition events in present-day and future high-resolution global simulations," J. Clim. **34**(12), 5037–5062 (2021).

Michaelis, A. C. and Lackmann, G. M., "Climatological changes in the extratropical transition of tropical cyclones in high-resolution global simulations," J. Clim. **32**, 8733–8753 (2019).

Minuzzi, F. C. and Farina, L., "A deep learning approach to predict significant wave height using long short-term memory," Ocean Model. **181**, 102151 (2023).

Mishnaevsky, L., Hasager, C. B., Bak, C., Tilg, A.-M., Bech, J. I., Rad, S. D., and Faester, S., "Leading edge erosion of wind turbine blades: Understanding, prevention and protection," Renewable Energy **169**, 953–969 (2021).

Mogensen, K. S., Magnusson, L., Mishnaevsky, and Bidlot, J.-R., "Tropical cyclone sensitivity to ocean coupling in the ECMWF coupled model," J. Geophys. Res. Oceans **122**, 4392–4412, https://doi.org/10.1002/2017JC012753 (2017).

Montgomery, M. T. and Smith, R. K., "Recent developments in the fluid dynamics of tropical cyclones," Annu. Rev. Fluid Mech. **49**(1), 541–574 (2017).

Moon, I. J., Knutson, T. R., Kim, H. J., Babanin, A. V., and Jeong, J. Y., "Why do eastern North Pacific hurricanes intensify more and faster than their western-counterpart typhoons with less ocean energy?," Bull. Am. Meteorol. Soc. **103**(11), E2604–E2627 (2022).

Musial, W., Beiter, P., Stefek, J., Scott, G., Heimiller, D., Stehly, T., Tegen, S., Roberts, O., Greco, T., and Keyser, D., "Offshore wind in the US Gulf of Mexico: Regional economic modeling and site-specific analyses," Report No. BOEM 2020-018 (Bureau of Ocean Energy Management, New Orleans, LA, 2020), p. 99.

Merizzi, F., Asperti, A., and Colamonaco, S., "Wind speed super-resolution and validation: From ERA5 to CERRA via diffusion models," arXiv:2401.15469 (2024).

Nguyen, T., Brandstetter, J., Kapoor, A., Gupta, J. K., and Grover, A., "Climax: A foundation model for weather and climate," arXiv:2301.10343 (2023).

NOAA, see https://sciencecouncil.noaa.gov/wp-content/uploads/2023/05/1.1_SOS_Atlantic_Hurricanes_Climate.pdf for NOAA Technical Report (2023).

O'Grady, J. G., Stephenson, A. G., and McInnes, K. L., "Gauging mixed climate extreme value distributions in tropical cyclone regions," Sci. Rep. **12**, 4626 (2022).

Olabarrieta, M., Medina, R., and Castanedo, S., "Effects of wave-current interaction on the current profile," Coastal Eng. **57**(7), 643–655 (2010).

Olabarrieta, M., Warner, J. C., Armstrong, B., Zambon, J. B., and He, R., "Ocean–atmosphere dynamics during Hurricane Ida and Nor'Ida: An application of the coupled ocean–atmosphere–wave–sediment transport (COAWST) modeling system," Ocean Modell. **43–44**, 112–137 (2012).

Oost, W. A., Komen, G. J., Jacobs, C. M. J., and Van Oort, C., "New evidence for a relation between wind stress and wave age from measurements during ASGAMAGE," Boundary-Layer Meteorol. **103**(3), 409–438 (2002).

Ooyama, K. V., "A thermodynamic foundation for modeling the moist atmosphere," J. Atmos. Sci. **47**(21), 2580–2593 (1990).

Palmer, T., "Climate forecasting: Build high-resolution global climate models," Nature **515**(7527), 338–339 (2014).

Papin, P. P., Bosart, L. F., and Tom, R. D., "A feature-based approach to classifying summertime potential vorticity streamers linked to Rossby wave breaking in the North Atlantic Basin," J. Clim. **33**, 5953–5969 (2020).

Pathak, J., Subramanian, S., Harrington, P., Raja, S., Chattopadhyay, A., Mardani, M., Kurth, T., Hall, D., Li, Z., Azizzadenesheli, K., and Hassanzadeh, P., "FourCastNet: A global data-driven high-resolution weather model using adaptive Fourier neural operators," arXiv:2202.11214 (2022).

Perrie, W., Andreas, E. L., Zhang, W., Li, W., Gyakum, J., and McTaggart-Cowan, R., "Sea spray impacts on intensifying midlatitude cyclones," J. Atmos. Sci. **62**(6), 1867–1883 (2005).

Perrie, W., Ren, X., Zhang, W., and Long, Z., "Simulation of extratropical Hurricane Gustav using a coupled atmosphere-ocean-sea spray model," Geophys. Res. Lett. **31**(3), L03110, https://doi.org/10.1029/2003GL018571 (2004).

Pleskachevsky, A., Dobrynin, M., Babanin, A. V., Günther, H., and Stanev, E., "Turbulent mixing due to surface waves indicated by remote sensing of suspended particulate matter and its implementation into coupled modeling of waves, turbulence, and circulation," J. Phys. Oceanogr. **41**(4), 708–724 (2011).

Porchetta, S., Temel, O., Muñoz-Esparza, D., Reuder, J., Monbaliu, J., van Beeck, J., and van Lipzig, N., "A new roughness length parameterization accounting for wind-wave (mis)alignment," Atmos. Chem. Phys. **19**(10), 6681–6700 (2019).

Porchetta, S., Temel, O., Warner, J. C., Muñoz-Esparza, D., Monbaliu, J., van Beeck, J., and van Lipzig, N., "Evaluation of a roughness length parametrization accounting for wind–wave alignment in a coupled atmosphere–wave model," Q. J. R. Meteorol. Soc. **147**(735), 825–846 (2021).

Powers, J. G., Klemp, J. B., Skamarock, W. C., Davis, C. A., Dudhia, J., Gill, D. O., Coen, J. L., Gochis, D. J., Ahmadov, R., Peckham, S. E., Grell, G. A., Michalakes, J., Trahan, S., Benjamin, S. G., Alexander, C. R., Dimego, G. J., Wang, W., Schwartz, C. S., Romine, G. S. *et al.*, "The weather research and forecasting model: Overview, system efforts, and future directions," Bull. Am. Meteorol. Soc. **98**(8), 1717–1737 (2017).

Pradhan, R., Aygun, R. S., Maskey, M., Ramachandran, R., and Cecil, D. J., "Tropical cyclone intensity estimation using a deep convolutional neural network," IEEE Trans. Image Process. **27**, 692–702 (2018).

Prakash, K. R., Pant, V., and Nigam, T., "Effects of the sea surface roughness and sea spray-induced flux parameterization on the simulations of a tropical cyclone," J. Geophys. Res. **124**(24), 14037–14058, https://doi.org/10.1029/2018JD029760 (2019).

Pringle, W. J., Wang, J., Roberts, K. J., and Kotamarthi, V. R., "Projected changes to cool-season storm tides in the 21st century along the Northeastern United States Coast," Earth's Future **9**(7), e2020EF001940 (2021).

Pringle, W. J. and Kotamarthi, V. R., "Coupled ocean wave-atmosphere models for offshore wind energy applications," Report No. ANL/EVS-21/8, 2021.

Pryor, S. C., Barthelmie, R. J., Cadence, J., Dellwik, E., Hasager, C. B., Kral, S. T., Reuder, J., Rodgers, M., and Veraart, M., "Atmospheric drivers of wind turbine blade leading edge erosion: review and recommendations for future research," Energies **15**, 8553 (2022).

Qiao, F., Song, Z., Bao, Y., Song, Y., Shu, Q., Huang, C., and Zhao, W., "Development and evaluation of an Earth System Model with surface gravity waves," J. Geophys. Res. **118**(9), 4514–4524, https://doi.org/10.1002/jgrc.20327 (2013).

Qiao, F., Yuan, Y., Yang, Y., Zheng, Q., Xia, C., and Ma, J., "Wave-induced mixing in the upper ocean: Distribution and application to a global ocean circulation model," Geophys. Res. Lett. **31**(11), L11303, https://doi.org/10.1029/2004GL019824 (2004).
Rendfrey, T. S., Bukovsky, M. S., McCrary, R. R., and Fuentes-Franco, R., "An assessment of tropical cyclones in North American CORDEX WRF simulations," Weather Clim. Extremes **34**, 100382 (2021).
Reed, K. A. and Jablonowski, C., "Assessing the uncertainty in tropical cyclone simulations in NCAR's community atmosphere model," J. Adv. Model. Earth Syst. **3**(3), M08002 (2011).
Reed, K. A., Bacmeister, J. T., Huff, J. J. A., Wu, X., Bates, S. C., and Rosenbloom, N. A., "Exploring the impact of dust on North Atlantic hurricanes in a high-resolution climate model," Geophys. Res. Lett. **46**, 1105–1112, https://doi.org/10.1029/2018GL080642 (2019).
Ren, H., Dudhia, J., and Li, H., "Large-eddy simulation of idealized hurricanes at different sea surface temperatures," J. Adv. Model. Earth Syst. **12**(9), e2020MS002057 (2020).
Ren, H., Dudhia, J., Shitang, K., and Li, H., "The basic wind characteristics of idealized hurricanes of different intensity levels," J. Wind Eng. Ind. Aerodyn. **225**, 104980 (2022).
Reichl, B. G., Hara, T., and Ginis, I., "Sea state dependence of the wind stress over the ocean under hurricane winds," J. Geophys. Res. **119**(1), 30–51, https://doi.org/10.1002/2013JC009289 (2014).
Resio, D. T. and Westerink, J. J., "Modeling the physics of storm surges," Phys. Today **61**(9), 33–38 (2008).
Ricciardulli, L. and Howell, B., see https://community.wmo.int/en/iwtc-10-reports for "Topic 1.1: Remote sensing and TC analysis: Current and emerging satellite sensors" (2022).
Richter, D. H. and Stern, D. P., "Evidence of spray-mediated air-sea enthalpy flux within tropical cyclones," Geophys. Res. Lett. **41**(8), 2997–3003, https://doi.org/10.1002/2014GL059746 (2014).
Roberts, M. J., Camp, J., Seddon, J., Vidale, P. L., Hodges, K., Vannière, B. *et al.*, "Projected future changes in tropical cyclones using the CMIP6 HighResMIP multimodel ensemble," Geophys. Res. Lett. **47**(14), e2020GL088662, https://doi.org/10.1029/2020GL088662 (2020).
Roberts, M. J., Vidale, P. L., Mizielinski, M. S., Demory, M. E., Schiemann, R., Strachan, J., Hodges, K., Bell, R., and Camp, J., "Tropical cyclones in the UPSCALE ensemble of high-resolution global climate models," J. Clim. **28**(2), 574–596 (2015).
Roberts, M. J., Camp, J., Seddon, J., Vidale, P. L., Hodges, K., Vanniere, B. *et al.*, "Impact of model resolution on tropical cyclone simulation using the HighResMIP-PRIMAVERA multimodel ensemble," J. Clim. **33**(7), 2557–2583 (2020).
Rodysill, J. R., Donnelly, J. P., Sullivan, R., Lane, P. D., Toomey, M., Woodruff, J. D. *et al.*, "Historically unprecedented Northern Gulf of Mexico hurricane activity from 650 to 1250 CE," Sci. Rep. **10**(1), 19092 (2020).
Rose, S., Jaramillo, P., Small, M. J., Grossmann, I., and Apt, J., "Quantifying the hurricane risk to offshore wind turbines," Proc. Nat. Acad. Sci. U. S. A. **109**(9), 3247–3252 (2012).
Rotunno, R., Chen, Y., Wang, W., Davis, C., Dudhia, J., and Holland, G. J., "Large-eddy simulation of an idealized tropical cyclone," Bull. Am. Meteorol. Soc. **90**(12), 1783–1788 (2009).
Sanchez Gomez, M., Lundquist, J. K., Deskos, G., Arwade, S. R., Meyers, A. T., and Hajjar, J. F., "Wind conditions in category 1–3 tropical cyclones can exceed wind turbine design standards," J. Geophys. Res. **128**, e2023JD039233, https://doi.org/10.1029/2023JD039233 (2023).
Schaffer, J. D., Roebber, P. J., and Evans, C., "Development and evaluation of an evolutionary programming-based tropical cyclone intensity model," Mon. Weather Rev. **148**, 1951–1970 (2020).
Schneider, T., Teixeira, J., Bretherton, C. S., Brient, F., Pressel, K. G., Schär, C., and Siebesma, A. P., "Climate goals and computing the future of clouds," Nat. Clim. Change **7**(1), 3–5 (2017).
Shaevitz, D. A., Camargo, S. J., Sobel, A. H., Jonas, J. A., Kim, D., Kumar, A. *et al.*, "Characteristics of tropical cyclones in high-resolution models in the present climate," J. Adv. Model. Earth Syst. **6**(4), 1154–1172 (2014).
Shchepetkin, A. F. and McWilliams, J. C., "The regional oceanic modeling system (ROMS): A split-explicit, free-surface, topography-following-coordinate oceanic model," Ocean Modell. **9**(4), 347–404 (2005).
Shchepetkin, A. F. and McWilliams, J. C., "Correction and commentary for "Ocean forecasting in terrain-following coordinates: Formulation and skill assessment of the regional ocean modeling system" by Haidvogel *et al.*, J. Comp. Phys. 227, pp. 3595–3624," J. Comput. Phys. **228**(24), 8985–9000 (2009).
Shimura, T., Mori, N., Takemi, T., and Mizuta, R., "Long-term impacts of ocean wave-dependent roughness on global climate systems," J. Geophys. Res. **122**(3), 1995–2011, https://doi.org/10.1002/2016JC012621 (2017).
Siddons, C., Macleod, C., Yang, L., and Stack, M., "An experimental approach to analysing rain droplet impingement on wind turbine blade materials," in EWEA 2015 Annuual Event (2015).
Skamarock, W. C., Klemp, J. B., Dudhia, J., Gill, D. O., Barker, D. M., Wang, W., and Powers, J. G., "A description of the advanced research WRF version 2," Report No. NCAR/TN-468+STR (University Corporation for Atmospheric Research, 2005).
Smith, J. A., "Wave–current interactions in finite depth," J. Phys. Oceanogr. **36**(7), 1403–1419 (2006).
Snaiki, R. and Wu, T., "Knowledge-enhanced deep learning for simulation of tropical cyclone boundary-layer winds," J. Wind Eng. Ind. Aerodyn. **194**, 103983 (2019).
Song, T., Han, R., Meng, F., Wang, J., Wei, W., and Peng, S., "A significant wave height prediction method based on deep learning combining the correlation between wind and wind waves," Front. Mar. Sci. **9**, 7 (2022).
Song, Y., Qiao, F., and Song, Z., "Improved simulation of the South Asian summer monsoon in a coupled GCM with a more realistic ocean mixed layer," J. Atmos. Sci. **69**(5), 1681–1690 (2012).
Staid, A., Pinson, P., and Guikema, S. D., "Probabilistic maximum-value wind prediction for offshore environments," Wind Energy **18**(10), 1725–1738 (2015).
Stengel, K., Glaws, A., Hettinger, D., and King, R. N., "Adversarial super-resolution of climatological wind and solar data," Proc. Natl. Acad. Sci. **117**(29), 16805–16815 (2020).
Stern, D. P., Bryan, G. H., and Aberson, S. D., "Extreme low-level updrafts and wind speeds measured by dropsondes in tropical cyclones," Mon. Weather Rev. **144**(6), 2177–2204 (2016).
Stern, D. P., Bryan, G. H., Lee, C.-Y., and Doyle, J. D., "Estimating the risk of extreme wind gusts in tropical cyclones using idealized large-eddy simulations and a statistical–dynamical model," Mon. Weather Rev. **149**, 4183–4204 (2021).
Strong, J. D. O., Vecchi, G. A., and Ginoux, P., "The climatological effect of Saharan dust on global tropical cyclones in a fully coupled GCM," J. Geophys. Res. **123**, 5538–5559, https://doi.org/10.1029/2017JD027808 (2018).
Sullivan, P. P. and McWilliams, J. C., "Dynamics of winds and currents coupled to surface waves," Annu. Rev. Fluid Mech. **42**(1), 19–42 (2010).
Sun, Q., Song, J., and Guan, C., "Simulation of the ocean surface mixed layer under the wave breaking," Acta Oceanol. Sin. **24**(3), 9–15 (2005).
Tan, J., Yang, Q., Hu, J., Huang, Q., and Chen, S., "Tropical cyclone intensity estimation using Himawari-8 satellite cloud products and deep learning," Remote Sens. **14**, 812 (2022).
Tang, J., Zhang, J. A., Chan, P., Hon, K., Lei, X., and Wang, Y., "A direct aircraft observation of helical rolls in the tropical cyclone boundary layer," Sci. Rep. **11**, 18771 (2021).
Tao, S., Zhang, X., Wang, Y., and Yang, J., "Transient behavior analysis of offshore wind turbines during lightning strike to multi-blade," IEEE Access **6**, 22070–22083 (2018).
Taylor, P. K. and Yelland, M. J., "The dependence of sea surface roughness on the height and steepness of the waves," J. Phys. Oceanogr. **31**(2), 572–590 (2001).
Terray, E. A., Donelan, M. A., Agrawal, Y. C., Drennan, W. M., Kahma, K. K., Williams, A. J., Hwang, P. A., and Kitaigorodskii, S. A., "Estimates of kinetic energy dissipation under breaking waves," J. Phys. Oceanogr. **26**(5), 792–807 (1996).
Tian, J. and Ma, K.-K., "A survey on super-resolution imaging," Signal Image Video Process. **5**, 329–342 (2011).
Tian, W., Zhou, X., Niu, X., Lai, L., Zhang, Y., and Sian, K. T. C. L. K., "A lightweight multitask learning model with adaptive loss balance for tropical cyclone intensity and size estimation," IEEE J. Sel. Top. Appl. Earth Obs. Remote Sens. **16**, 1057–1071 (2023).
Toba, Y. and Kawamura, H., "Wind-wave coupled downward-bursting boundary layer (DBBL) beneath the sea surface," J. Oceanogr. **52**(4), 409–419 (1996).

Toffoli, A., McConochie, J., Ghantous, M., Loffredo, L., and Babanin, A. V., "The effect of wave-induced turbulence on the ocean mixed layer during tropical cyclones: Field observations on the Australian North-West Shelf," J. Geophys. Res. **117**(C11), C00J24, https://doi.org/10.1029/2011JC007780 (2012).

Toomey, M. R., Curry, W. B., Donnelly, J. P., and Van Hengstum, P. J., "Reconstructing 7000 years of North Atlantic hurricane variability using deep-sea sediment cores from the western Great Bahama Bank," Paleoceanography **28**(1), 31–41, https://doi.org/10.1002/palo.20012 (2013).

Touma, D., Stevenson, S., Camargo, S. J., Horton, D. E., and Diffenbaugh, N. S., "Variations in the intensity and spatial extent of tropical cyclone precipitation," Geophys. Res. Lett. **46**(23), 13992–14002, https://doi.org/10.1029/2019GL083452 (2019).

Tsartsali, E. E., Haarsma, R. J., Athanasiadis, P. J., Bellucci, A., de Vries, H., Drijfhout, S., de Vries, I. E., Putrahasan, D., Roberts, M. J., Sanchez–Gomez, E., and Roberts, C. D., "Impact of resolution on the atmosphere–ocean coupling along the Gulf Stream in global high resolution models," Clim. Dyn. **58**(11–12), 3317–3333 (2022).

Ulbrich, U., Leckebusch, G. C., and Pinto, J. G., "Extra-tropical cyclones in the present and future climate: A review," Theor. Appl. Climatol. **96**(1–2), 117–131 (2009).

Umlauf, L. and Burchard, H., "A generic length-scale equation for geophysical turbulence models," J. Mar. Res. **61**(2), 235–265 (2003).

Valcke, S., Craig, T., and Coquart, L., see http://www.cerfacs.fr/oa4web/oasis3-mct_3.0/oasis3mct_UserGuide.pdf for "OASIS3-MCT_3.0 Coupler User Guide" (CER- FACS/CNRS, Toulouse, France, 2015), p. 58; accessed Aug 1 2023.

Varalakshmi, P., Vasumathi, N., and Venkatesan, R., "Tropical cyclone intensity prediction based on hybrid learning techniques," J. Earth Syst. Sci. **132**, 28 (2023).

Varlas, G., Vervatis, V., Spyrou, C., Papadopoulou, E., Papadopoulos, A., and Katsafados, P., "Investigating the impact of atmosphere–wave–ocean interactions on a Mediterranean tropical-like cyclone," Ocean Modell. **153**, 101675 (2020).

Vecchi, G. A., Landsea, C., Zhang, W., Villarini, G., and Knutson, T., "Changes in Atlantic major hurricane frequency since the late-19th century," Nat. Commun. **12**, 4054 (2021).

Vickery, P. J., Skerlj, P. F., and Twisdale, L. A., "Simulation of hurricane risk in the U.S. using empirical track model," J. Struct. Eng. **126**(10), 1222–1237 (2000).

Vitart, F., Ardilouze, C., Bonet, A., Brookshaw, A., Chen, M., Codorean, C. *et al.*, "The subseasonal to seasonal (S2S) prediction project database," Bull. Am. Meteorol. Soc. **98**(1), 163–173 (2017).

Wada, A. and Usui, N., "Impacts of oceanic preexisting conditions on predictions of Typhoon Hai-Tang in 2005," Adv. Meteorol. **2010**, 756071 (2010).

Wada, A., Kanada, S., and Yamada, H., "Effect of air-sea environmental conditions and interfacial processes on extremely intense Typhoon Haiyan," J. Geophys. Res. **123**(405), 379–310 (2018).

WAMDI Group, "The WAM model—A third generation ocean wave prediction model," J. Phys. Oceanogr. **18**(12), 1775–1810 (1988).

Wang, J. *et al.*, "Impact of tropical and extratropical cyclones on future U.S. Offshore Wind Energy," Bull. Am. Meteorol. Soc. **105**, E1506–E1513 (2024).

Wang, Y. Q. and Wu, C. C., "Current understanding of tropical cyclone structure and intensity changes–A review," Meteorol. Atmos. Phys. **87**(4), 257–278 (2004).

Wang, Y., Qiao, F., Fang, G., and Wei, Z., "Application of wave-induced vertical mixing to the K profile parameterization scheme," J. Geophys. Res. **115**(9), 1–12, https://doi.org/10.1029/2009JC005856 (2010).

Warner, J. C., Armstrong, B., He, R., and Zambon, J. B., "Development of a coupled ocean-atmosphere-wave-sediment transport (COAWST) modeling system," Ocean Modell. **35**(3), 230–244 (2010).

Warner, J. C., Sherwood, C. R., Signell, R. P., Harris, C. K., and Arango, H. G., "Development of a three-dimensional, regional, coupled wave, current, and sediment-transport model," Comput. Geosci. **34**(10), 1284–1306 (2008).

Wehner, M. F., Reed, K. A., Li, F., Prabhat, Bacmeister, J., Chen, C. T., Jablonowski, C. *et al.*, "The effect of horizontal resolution on simulation quality in the Community Atmospheric Model, CAM5.1," J. Adv. Model. Earth Syst. **6**(4), 980–997 (2014).

Wei, Z., "Forecasting wind waves in the US Atlantic Coast using an artificial neural network model: Towards and AI-based storm forecast system," Ocean Eng. **237**, 109646 (2021).

Wimmers, A. and Duong, Q.-P., https://community.wmo.int/en/iwtc-10-reports for "Topic 1.2: Objective satellite methods including AI algorithms" (2022).

Wimmers, A., Velden, C., and Cossuth, J. H., "Using deep learning to estimate tropical cyclone intensity from satellite passive microwave imagery," Mon. Weather Rev. **147**, 2261–2282 (2019).

Worsnop, R. P., Bryan, G. H., Lundquist, J. K., and Zhang, J. A., "Using large-eddy simulations to define spectral and coherence characteristics of the hurricane boundary layer for wind-energy applications," Boundary-Layer Meteorol. **165**(1), 55–86 (2017a).

Worsnop, R. P., Lundquist, J. K., Bryan, G. H., Damiani, R., and Musial, W., "Gusts and shear within hurricane eyewalls can exceed offshore wind turbine design standards," Geophys. Res. Lett. **44**, 6413–6420, https://doi.org/10.1002/2017GL073537 (2017b).

Wu, L., Breivik, Ø., and Rutgersson, A., "Ocean-wave-atmosphere interaction processes in a fully coupled modeling system," J. Adv. Model. Earth Syst. **11**(11), 3852–3874 (2019).

Wu, L., Shao, M., and Sahlée, E., "Impact of air-wave-sea coupling on the simulation of offshore wind and wave energy potentials," Atmosphere **11**(4), 1–21 (2020).

Xu, J., Wang, X., Wan, H., Zhao, C., Wang, H., and Zhu, J., "Tropical cyclone size estimation based on deep learning using infrared and microwave satellite data," Front. Mar. Sci. **9**, 1077901 (2022).

Yamaguchi, M., Ishida, J., Sato, H., and Nakagawa, M., "WGNE intercomparison of tropical cyclone forecasts by operational NWP models: A quarter century and beyond," Bull. Am. Meteorol. Soc. **98**(11), 2337–2349 (2017).

Yan, D. and Zhang, T., "Research progress on tropical cyclone parametric wind-field models and their application," Reg. Stud. Mar. Sci. **51**(2022), 102207 (2022).

Yang, C.-Y., Ma, C., and Yang, M.-H., "Single-image super-resolution: A benchmark," in *Computer Vision – ECCV 2014*, Lecture Notes in Computer Science Vol. 8692, edited by Fleet, D., Pajdla, T., Schiele, B., and Tuytelaars, T. (Springer, Cham, 2014).

Yang, Q., Lee, C.-Y., Tippett, M. K., Chavas, D. R., and Knutson, T. R., "Machine learning-based hurricane wind reconstruction," Weather Forecast. **37**, 477–493 (2022).

Yuan, Y. L., Hua, F., and Pan, Z. D., "LAGFD-WAM numerical wave model-I. Basic physical model," Acta Oceanol. Sin. **10**(4), 483–488 (1991).

Yuan, Y. L., Hua, F., and Pan, Z. D., "LAGFD-WAM numerical wave model-II. Characteristics inlaid scheme and its application," Acta Oceanol. Sin. **11**(1), 13–23 (1992).

Zambon, J. B., He, R., Warner, J. C., and Hegermiller, C. A., "Impact of SST and surface waves on hurricane florence (2018): A coupled modeling investigation," Weather Forecast. **36**(5), 1713–1734 (2021).

Zhang, G., Wang, Z., Dunkerton, T. J., Peng, M. S., and Magnusdottir, G., "Extratropical impacts on atlantic tropical cyclone activity," J. Atmos. Sci. **73**, 1401–1418 (2016).

Zhang, J., Huang, L., Wen, Y., and Deng, J., "A distributed coupled atmosphere-wave-ocean model for typhoon wave numerical simulation," Int. J. Comput. Math. **86**(12), 2095–2103 (2009a).

Zhang, J. A., Drennan, W. M., Black, P. G., and French, J. R., "Turbulence structure of the hurricane boundary layer between the outer rainbands," J. Atmos. Sci. **66**(8), 2455–2467 (2009b).

Zhang, J. A., Atlas, R., Emmitt, G. D., Bucci, L., and Ryan, K., "Airborne Doppler wind Lidar observations of the tropical cyclone boundary layer," Remote Sens. **10**, 825 (2018).

Zhang, R. and Shen, X., "On the development of the GRAPES – A new generation of the national operational NWP system in China, Chinese," Sci. Bull. **53**, 3429–3432 (2008).

Zhang, S., Xu, S., Fu, H., Wu, L., Liu, Z., Gao, Y. *et al.*, "Toward Earth system modeling with resolved clouds and ocean submesoscales on heterogeneous many-core HPCs," Nat. Sci. Rev. **10**(6), nwad069 (2023a).

Zhang, S., Yuan, Y., and Zheng, Q., "Modeling of the eddy viscosity by breaking waves," Acta Oceanol. Sin. **26**(6), 116–123 (2007).

Zhang, W., Zhang, J., Liu, Q., Sun, J., Li, R., and Guan, C., "Effects of surface wave-induced mixing and wave-affected exchange coefficients on tropical cyclones," Remote Sens. **15**(6), 1594 (2023b).

Zhang, W., Zhao, D., Zhu, D., Li, J., Guan, C., and Sun, J., "A numerical investigation of the effect of wave-induced mixing on tropical cyclones using a coupled ocean-atmosphere-wave model," J. Geophys. Res. **127**(13), 1–23, https://doi.org/10.1029/2021JD036290 (2022).

Zhao, B., Qiao, F., Cavaleri, L., Wang, G., Bertotti, L., and Liu, L., "Sensitivity of typhoon modeling to surface waves and rainfall," J. Geophys. Res. **122**(3), 1702–1723, https://doi.org/10.1002/2016JC012262 (2017).

Zhao, B., Wang, G., Zhang, J. A., Liu, L., Liu, J., Xu, J., Yu, H., Zhao, C., Yu, X., Sun, C., and Qiao, F., "The effects of ocean surface waves on tropical cyclone intensity: Numerical simulations using a regional atmosphere-ocean-wave coupled model," J. Geophys. Res. **127**(11), e2022JC019015, https://doi.org/10.1029/2022JC019015 (2022).

Zhu, G., Li, Q., Zhao, W., Ly, X., Qian, C., and Qian, Q., "Tropical cyclones intensity prediction in the Western North Pacific using gradient boosted regression tree model," Front. Earth Sci. **10**, 929115 (2022).

Zhuo, J.-Y. and Tan, Z.-M., "Physics-augmented deep learning to improve tropical cyclone intensity and size estimation from satellite imagery," Mon. Weather Rev. **140**, 2097–2113 (2021).